Universidade de Aveiro
2021

JOANA MARIA MOREIRA PEREIRA

Evaluation of *in vitro* biocompatibility of functionalized magnesium alloys for application in orthopedic implants

Avaliação *in vitro* da biocompatibilidade de ligas de magnésio funcionalizadas para aplicações como implantes ortopédicos

Universidade de Aveiro
2021

Joana Maria Moreira Pereira

Evaluation of *in vitro* biocompatibility of functionalized magnesium alloys for application in orthopedic implants

Dissertation submitted to the University of Aveiro to fulfil the requirements for obtaining a master's degree in Materials and Biomedical Devices, held under the scientific guidance of Prof. João Tedim, assistant professor at the Department of Materials and Ceramic Engineering, University of Aveiro, Dr. Isabel Sousa, researcher at SECoP at CICECO, University of Aveiro and Dr. Sónia Fraga, researcher at the National Institute of Health Dr. Ricardo Jorge.

This work was partially supported by Fundação para a Ciência e Tecnologia I.P. (FCT, IP) through the project PTDC/CTM-BIO/2170/2014.

The jury

President

Doctor Filipe José Alves de Oliveira
Principal Investigator in Labor Regime, University of Aveiro

Doctor Tânia Alexandra Fernandes de Sousa Moniz Abreu
Junior Researcher, REQUIMTE-LAQV, Department of Applied Chemistry, Faculty of Pharmacy, University of Porto

Doctor Isabel Cristina de Sá Correia de Sousa
PhD Researcher (level 1), University of Aveiro

acknowledgments

I would like to express sincere gratitude to Prof. João Tedim, Dr. Isabel Sousa and Dr. Sónia Fraga for their guidance, encouragement and expertise during some particular unusual times. I would also like to address my appreciation to everyone from SECoP group for the generous way they received me, and for their availability and willingness to help, in particular to Dr. Isabel Sousa, for all of her teachings, patience and guidance. I would also like to acknowledge the people from ISPUP that contributed to this project and generously received me, in particular to Dr. Sónia Fraga, that during an emerging new situation, with new restrictions found solutions to guarantee that I was able to continue the work. Last but not least, to my parents, sister, and my closest friends, who have always supported and encourage me for the last years, thank you.

palavras-chave

ligas de magnésio, propriedades anti corrosão, aplicações ortopédicas, citotoxicidade, hemocompatibilidade.

resumo

As ligas de magnésio têm sido amplamente estudadas e aplicadas no campo da biomedicina, nomeadamente na área ortopédica, devido às suas propriedades promissoras. A biocompatibilidade, biodegradabilidade, propriedades mecânicas e osteogénicas destas ligas, permitem o seu uso como alternativas aos materiais atualmente disponíveis. No entanto, a corrosão descontrolada e a formação de hidrogénio, nas ligas de magnésio, podem causar sérios danos quando introduzidas no corpo humano. Para enfrentar estes desafios, diferentes métodos foram desenvolvidos de forma a controlá-los, como pré-tratamentos de superfície, revestimentos e diferentes elementos de liga. Os diferentes sistemas produzidos, no entanto, requerem uma avaliação detalhada da sua biocompatibilidade para uso posterior na área médica. Porém, existe uma lacuna na avaliação da biocompatibilidade, principalmente na hemocompatibilidade destes materiais. Este trabalho foi realizado no âmbito do projeto MAGICOAT e teve como objetivo avaliar a biocompatibilidade (citotoxicidade e hemocompatibilidade) de um sistema multicamada composto por uma liga de Mg1Ca, pré-tratada com hidroxiapatite, e um revestimento, subsequente, de poliéterimida (PEI) contendo microcápsulas de gelatina com cálcio ou partículas de carbonato de cálcio. Como as microcápsulas de gelatina carregadas de cálcio e as partículas de carbonato de cálcio deveriam ser incluídas no revestimento PEI, a sua morfologia, perfil de libertação de cálcio e sua citotoxicidade foram avaliadas antes dos ensaios de biocompatibilidade do sistema completo. O sistema multicamada completo foi inicialmente testado relativamente à sua citotoxicidade, analisando-se a integridade da membrana celular e a proliferação celular, através dos ensaios de LDH e WST-1. Após os resultados comprovarem que o sistema multicamadas não era tóxico, foram realizados testes de hemocompatibilidade. Testes *in vitro* para verificar a ocorrência de hemólise e a ativação do sistema complemento confirmaram a hemocompatibilidade do sistema após 4 horas de contato com o sangue.

keywords

magnesium alloys, anti-corrosion properties, orthopedical applications, cytotoxicity, hemocompatibility.

abstract

Magnesium alloys have been widely studied and applied in the biomedical field, namely in the orthopedic area, due to their promising properties. Their biocompatibility, biodegradability, mechanical properties and osteogenic properties allow the use of these alloys as alternatives to the currently available materials. However, the uncontrolled corrosion and hydrogen formation in magnesium alloys can cause serious damages when introduced into the human body. In order to meet these challenges, different methods have been developed to control them, such as surface pre-treatments, coatings and alloying. The different systems produced, however, require a detailed assessment of biocompatibility for later use in the medical field. But there is still a gap in the assessment of biocompatibility, especially in the hemocompatibility of such materials. This work was conducted in the scope of the MAGICOAT project and aimed to assess the biocompatibility (cytotoxicity and hemocompatibility) of a multilayer system composed of a Mg1Ca alloy, pre-treated with hydroxyapatite, with a subsequent polyetherimide (PEI) coating containing calcium-loaded gelatin microcapsules or calcium carbonate particles. As both calcium-loaded gelatin microcapsules and calcium carbonate particles were to be included in the PEI coating, their morphology, release profile and their cytotoxicity were assessed prior to the biocompatibility assays of the complete system. The complete multilayer system was initially tested for cytotoxicity, analyzing the integrity of the cell membrane and cell proliferation, through LDH and WST-1 assays. After the results proved that the multilayer system was non-toxic, hemocompatibility tests were carried out. In vitro tests to verify the occurrence of hemolysis and activation of the complement system confirmed the hemocompatibility of the system after 4 hours of contact with the blood.

Table of contents

Abbreviations

8HQ - 8-hydroxyquinoline

ALP - Alkaline Phosphatase Assay

ATCC - American Type of culture collection

Ca@gel – Calcium-loaded gelatin microcapsules

$CaCO_3$ – Calcium carbonate particles

Ca-EDTA - Ethylenediaminetetraacetic acid calcium disodium salt hydrate

CaP – Calcium phosphate

DCM – Dichloromethane

DMEM - Dulbecco's Modified Eagle Medium.

ELISA - Enzyme-Linked Immunosorbent Assay

FDA - Food and Drugs Agency

GRAS - Generally regarded as safe material

HAp – Hydroxyapatite

Hb – Hemoglobin

HBSS - Hank's balanced salt solution

HiCN – Hemiglobincyanide

HZG - Helmholtz-Zentrum Geestacht

ISO – International Organization for Standardization

ISPUP – University of Porto Institute for Public Health

L929 - Fibroblast cell line

LDH - Lactate Deydrogenase release assay

MEM - Minimum Essential Medium Eagle

Mg alloys - Mg alloys

MTS- 3-(4,5-dimethylthiazol-2-yl)-5-(3-carboxymethoxyphenyl) - 2-(4-sulfophenyl)-2H-tetrazolium

MTT - 3-(4,5-dimethylthiazol-2-yl)-2,5-diphenyltetrazoliumbromide

PCL - Polycaprolactone

PEI – Polyetherimide

PI - Propidium Iodide assay

PLA - Polylactic acid

PLGA - Polylactic-co-glycolic acid

RBCs – Red blood cells

SBF – Stimulated Body Fluid

SEM - Scanning Electron Microscopy

WST-1 - Assay for Cell Proliferation and Viability

List of figures

List of tables

Chapter 0: Introduction

The present work was developed within the frame of the MAGICOAT- "Controlling the degradation of magnesium alloys for biomedical applications using innovative smart coatings" project (ref. PTDC/CTM-BIO/2170/2014). MAGICOAT's objective was to develop a multilayered coating system for the controlled degradation of magnesium alloys (Mg alloys) used in biomedical applications. Within this project, different magnesium alloys, pre-treatments, coatings and active species were assessed in terms of electrochemical behavior and cytotoxicity. A multilayer system emerged from this investigation, combining two layers, which showed the most promising results in electrochemical and cytotoxicity assays. The multilayer system is composed by an Mg1Ca alloy, pretreated with hydroxyapatite (HAp), with a polyetherimide (PEI) coating containing either calcium-loaded gelatin microcapsules (Ca@gel) or calcium carbonate particles ($CaCO_3$).

The biocompatibility evaluation of any material, to be considered as a material with a medical application, is of the uttermost importance, to guarantee no damage occurs when it is introduced in the human body.

Hence, the main aim of this work was to assess the biocompatibility (cytotoxicity and hemocompatibility) of the selected final multilayer system designed in the frame of MAGICOAT project. Prior to this, it was also necessary to characterize the morphology and release profile of the Ca@gel and $CaCO_3$ particles, as well as their cytotoxicity.

The present work is divided in 4 chapters. Chapter 1: State of art, presents the state of art, in which the relevant properties of the Mg alloys are presented and the reasons that make these alloys suitable replacements to the most used materials are exposed. The challenges still facing the application of these alloys are also described, as well as the solutions developed to overcome them. Chapter 1 also explores the biocompatibility testing for medical devices, exploring the recommended tests according to the respective classification in terms of medical devices. The main tests usually performed to assess cytotoxicity as well as hemocompatibility are exposed. Chapter 1 ends with the description of the most recent applications of Mg alloys in the orthopedical field.

In Chapter 2: Materials and methods, the materials and methods applied in the present work are described. The synthesis methodology of Ca@gel and $CaCO_3$ is described as well as their morphological characterization and release behavior experimental procedures. The cytotoxicity experimental procedure described extracts preparation, according to ISO 10993,

cell culture, test materials exposure and WST-1 and LDH release studies. Hemocompatibility was assessed by obtaining the hemolysis index as well as determining if the complement system was activated.

Chapter 3: Results and discussion presents all the results obtained and in which they are discussed. Chapter 3 is essentially divided in three parts, first the Ca@gel and $CaCO_3$ particles morphological characterization and calcium release profile followed by all biocompatibility results, from Ca@gel and $CaCO_3$ particles to the multilayer systems' cytotoxicity and hemocompatibility results.

In Chapter 4: Conclusion, the main observations and conclusions obtained from all the presented work are discussed, to determine if all the initial objectives were successfully achieved. Afterwards, in the future perspectives, some insights on how to improve the systems' biocompatibility and possible improvements are presented.

The present work was performed in collaboration with the Institute for Public Health (ISPUP) of the University of Porto where all the biocompatibility assays were conducted.

Chapter 1: State of Art

1.1. Introduction

In the field of biomedical materials, metals have been in the spotlight since the 1930s.[1] Due to their mechanical properties such as high tensile and yield strength, as well as resistance to fatigue and creep, they have been broadly studied and applied as orthopedical implants and stents. These characteristics make them superior to ceramics, polymer and polymer/ceramic composites.[2] Among these metals, stainless steel is one of the most common and the first to be used successfully.[1][3] Fracture fixation, stents and spinal implants are some of stainless steel applications as a biomaterial. Following the success of stainless steel, cobalt-chromium alloys and titanium alloys have also emerged. These three metal alloys are the most popular among metallic biomaterials. For instance, cobalt-chromium alloys can be used as stents but also in joint replacement, while titanium has applications in dental implants, fracture fixation as well as joint replacement applications, to name a few.[4]

However, most conventional metallic materials (e.g. stainless steel) have limitations and disadvantages associated with their use. They remain in the human body permanently, which might induce adverse reactions due to the release of toxic products through corrosion/wear processes.[5] In this context, biodegradable non-metal materials such as polymers, ceramics and bioactive glasses have been studied. These materials prevent the adverse effects that metallic implants are known to cause, as they can degrade *in vivo*, avoiding the permanent implantation and reducing the release of toxic products.[2] However, these biodegradable materials present very weak mechanical properties.[6] As an alternative, the traditional biodegradable metal implants seem an adequate solution but exhibit insufficient mechanical properties for bone implant applications or non-suitable degradation rates.[7]–[9]

Magnesium alloys (Mg alloys) seem to gather the best features of the two types of implants referred previously and have been widely studied and developed in industrial and biomedical fields.[9] Their advantages over traditional metals and biodegradable polymers (lightweight, low density, high strength/weight ratio), biocompatibility and *in vivo* importance [10] makes them suitable candidates for medical implants.[9] Their advantages make these alloys suitable for applications in the medical field such as in orthopedical and cardiovascular areas, as better alternatives to the traditional materials used in these sectors. Other areas where the potential of Mg alloys is being explored are maxillofacial, stomatology and sports medicine.[11]

Concerning cardiovascular-related applications, magnesium alloys are mostly used as cardiovascular stents. Until recently, the research in this area has focused its interest on three alloys: Fe-based, Zn-based and Mg-based. But among these three alloys, only Mg alloys have been already applied in clinical trials with good results. The use of stents as noninvasive and low-cost alternatives to the traditional techniques is what makes these magnesium-based stents a promising material.[12]

In the orthopedical area, the potential of Mg alloys, as a promising material in the treatment of different pathologies, was discovered and applied over a century ago. The first reports of Mg alloys used as implants in humans date to the early 1900s, where they were used on patients as bone fixators, in the treatment of fractures among other applications, as it can be seen in **Table 1**.[13]

Table 1 – Example of magnesium alloys applications and their outcomes in the last century.[14]

Year	Author	Type of application	Treatment	Follow-up
1900	Payer et al.	Bone pins and plates	Fixation of traumatic bones	———
1906	Lambut et al.	Mg plate and steel nail	Leg fracture of a 17-year-old	Subcutaneously inflated after 1 day. Accumulation of hydrogen due to galvanic corrosion.
1938	Mcbridge et al.	Screws, bolts and plates [Mg-Al-Mn]	20 fractures	No adverse reactions. Implants completely absorbed.
1948	Thortskii et al.	Plates and screws [Mg-Cd]	34 cases of pseudarthrosis	Successful replacement of the implant by new bone.

Even though the implant potential of these Mg alloys was undeniable, the lack of knowledge on techniques able to overcome implant failure, as well as some clinical complications caused by the implants, led to a halt on the development in this area.[13] In the orthopedical field, it was only in the last decade that the medical applications of these alloys emerged, once again, due to new advances in science and technologies (e.g. alloying, surface treatments and coatings techniques) capable of controlling the degradation rate of Mg

alloys.[13] This technological progress combined with magnesium alloys' properties, transformed these alloys into a biomaterial with great potential for orthopedical applications.[12]

1.2. Magnesium

Magnesium plays a major role in the human body as it is the fourth most abundant cation in the organism.[14] It exists in a bound and free ionized form and is a key element in several metabolic and biologic processes, being involved in hundreds of biochemical reactions.[15] Magnesium is present in human physiology and is essential to human metabolism. It is known for facilitating tissue healing and an excess of Mg^{2+} ions do not cause cellular toxicity and can be easily eliminated in urine.[16] The equilibrium between the absorption and excretion of Mg ions in the human body is schematically shown in **Figure 1**.

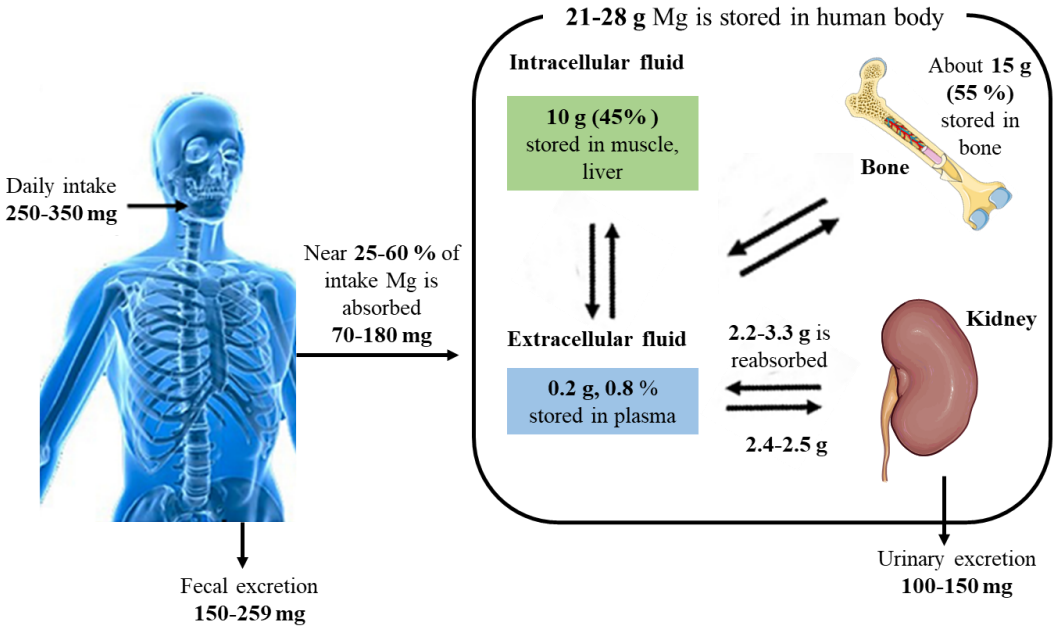

Figure 1 - Illustration of the dynamic equilibrium of Mg ions in the human body. Adapted from [13].

Good mechanical properties are fundamental for implants, in particular orthopedic implants, however, an exceeding stiffness of the traditional metallic implants can cause stress shielding and therefore, be harmful for the bone healing process.[16] Ultimately, stress shielding can decrease the stimuli to produce new bone growth and a reduction in bone remodulation which will lead to a less stable implant.[17]

When compared with other metallic, ceramic and polymeric materials used as orthopedic implants, magnesium presents mechanical properties, such as density, elastic modulus and yield strength, closer to those of natural bone,[18] as seen in **Figure 2**.

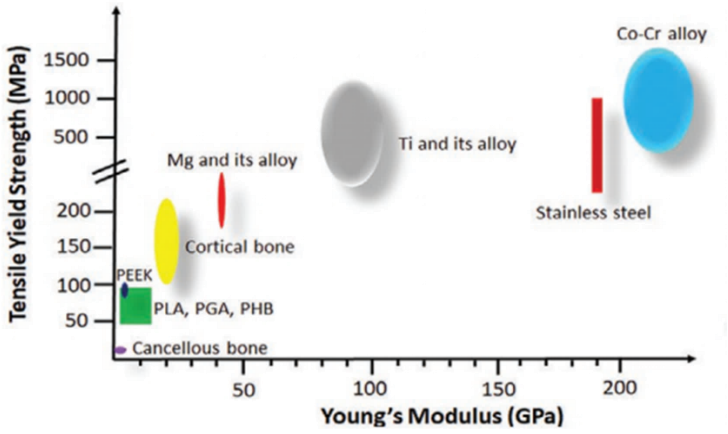

Figure 2 - Comparison of mechanical properties of different materials. Adapted from [18].

Natural bone presents a density of 1.8-2.1 g/cm^3, a yield strength of 130-180 MPa and an elastic modulus of 3-20 GPa, while magnesium alloys show a yield strength that varies from 85-190 MPa, an elastic modulus of 41-45 GPa [16] and a density of 1.74 g/cm^3.[19] This similarity shows that using magnesium alloys can reduce stress-shielding-related problems of orthopedic implants, for example, during the consolidation of a fracture.[18] Furthermore, the mechanical properties of magnesium alloys are superior to biodegradable synthetic polymers but inferior to permanent surgical steel or titanium alloys which is why, currently, magnesium alloys-based implants are only suitable for unload-bearing applications.[6] In order to broaden the applications of magnesium alloys as orthopedic implants, a further improvement of their mechanical properties is crucial.[17]

As mentioned previously, the biggest advantage of magnesium alloys is their biocompatibility. A biocompatible material must have an adequate biological response when introduced in the human body.[16] Magnesium and corresponding alloys have also been shown to promote osteogenesis, which is one of the conventional methods to evaluate the biocompatibility of a biomaterial.[1] Magnesium is essential to all living cells including osteoblasts and osteoclasts which the body needs for bone growth and repair.[20] It is the interaction between these bone cells that determines the remodeling process of bone. When magnesium decreases, bone cells react by decreasing and increasing the activity of the osteoblasts and osteoclasts, respectively.[21]

According to reported studies, where magnesium degradation exists there is greater bone mass and higher mineralization. There are also no adverse reactions from bone, joints and soft tissues to corroding magnesium.[22] Studies also show that slow corrosion leads to callus formation and, in some *in vivo* studies, the magnesium alloy stimulated bone formation and repressed bone resorption. This led to an increased formation of callus during fracture healing.[23] This callus functions as a connecting bridge along a bone fracture, during repair, making it an essential step in bone repair.[24]

Figure 3 represents the fluoroscopic images of polymeric and magnesium alloy-based implants. The polymer and magnesium alloys were implanted intramedullary into the femora of guinea pigs. It is possible to see bone growth in both implants. However, it was possible to observe ,around magnesium alloys, a higher increase in bone mass when compared to what was observed for the polymeric implant.[25]

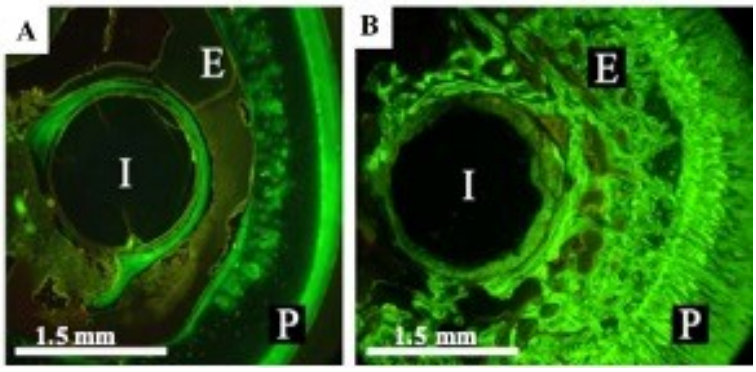

Figure 3 - Fluoroscopic images of cross-sections of (A) degradable polymer and (B) a magnesium rod. New bone formation was stained in vivo by calcein green. I = Implant residual P= periosteal bone formation E= endosteal bone formation. Adapted from [25].

Biodegradable implants such as magnesium and its alloys, dissolve in biological environments after a certain time of functional use.[3] Their biodegradability is possibly another great advantage. It avoids the need for a second surgery, becoming a cost-effective and convenient solution for patients by reducing, respectively, healthcare costs and patients morbidity, increasing the quality of life of the latter.[3] The ideal cycle expected of a biodegradable material implant, representing all stages in the material life cycle, is depicted in **Figure 4**.

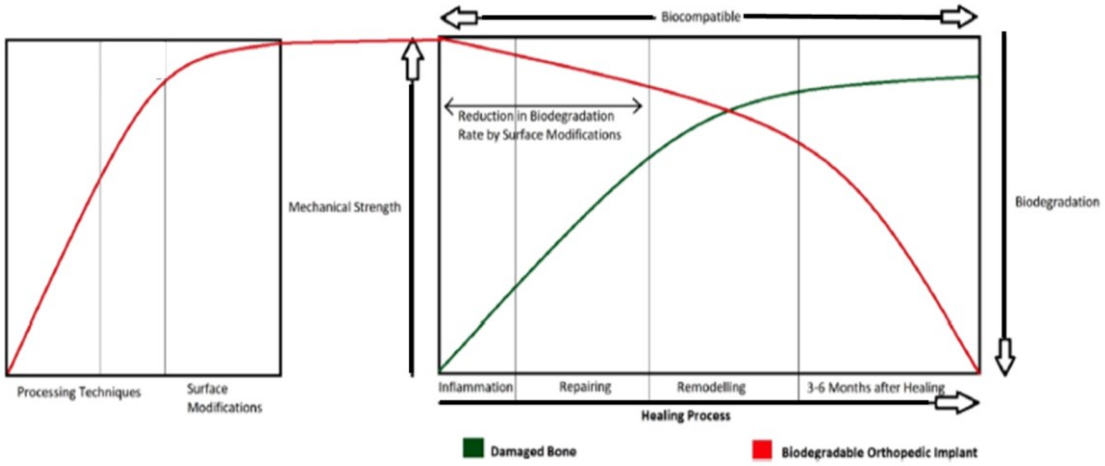

Figure 4 - Ideal cycle for a biodegradable material implant from preparation to complete disappearance. Adapted from [26].

Figure 4 shows the requirements in terms of biocompatibility, biodegradation and mechanical strength behavior for a biodegradable material to be considered ideal, as an implant material, in damaged bone. Maintaining a balance between a low corrosion rate, to allow the implant to guarantee support, and the bone healing rate is essential. The biodegradable implant should possess the ability to respond to the different mechanical properties required, during the healing process.[26]

It is expected for the implant to slowly start losing mechanical integrity and degrading, as the mechanical strength of the bone starts to increase, due to the formation of bone and cartilage. Thus, the ideal balance translates into an implant slowly degrading, while new bone is formed, consolidating the wound guaranteeing complete bone repair when total biodegradation occurs.[26] **Figure 5** shows the progressive degradation of a magnesium alloy-based biodegradable screw.

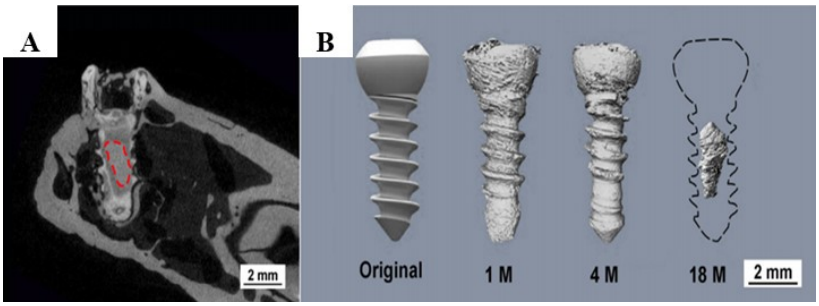

Figure 5 - 3D reconstruction of JDBM (Mg-2.8 wt%Nd-0.2 wt%Zn-0.4 wt%Zr alloy) screw after 18 months of implantation. (A) The red dashed marks the residual screw (B) original screw and the residual screw at 1,4 and 18 months after implantation. Adapted from [27].

Figure 5 presents the long-term degradation of a Mg alloy screw implanted in rabbit's mandibles. After 18 months, the JDBM screw showed good osteointegration and there was a 90 % decrease in screw volume, as observed in **Figure 5**, showing the potential use of these type of materials.[27]

However, despite the fact that degradation occurs in Mg alloys, the bone healing process (callus formation) takes up to 4 months to complete [28] and one of the major drawbacks, that has hindered the application of magnesium alloys as biomedical implants in a widespread manner, is their fast, uncontrolled and localized degradation by corrosion processes.[29]

1.3. Magnesium corrosion and hydrogen evolution

Corrosion is defined as "the destruction or deterioration of a material due to reaction with the environment, under the influence of chemical, physical and electrochemical factors".[30] However, magnesium corrosion, in the human body is more complex than in natural environments. The rate of corrosion in bodily fluids is affected by different factors such as the presence of proteins and pH, among others.

Magnesium has a negative electrochemical potential of -2.37 V.[31] Since body fluids have in their composition compounds such as oxygen and proteins, as well as aggressive species such as hydroxides and chlorides, magnesium might become very reactive. The free ions will travel from the metal surface into the surrounding environment. The corrosion reaction of magnesium is represented by equation 1.[29]

$$Mg + 2H_2O \rightarrow Mg(OH)_2 + H_2 \text{ (1)}$$

Equations 2 and 3 represent the half-reactions that occur, respectively, in the anode (oxidation) and cathode (reduction).

$$\text{(Oxidation reaction) } Mg \rightarrow Mg^{2+} + 2e^- \text{ (2)}$$

$$\text{(Reduction reaction) } 2H_2O + 2e^- \rightarrow H_2 + 2OH^- \text{ (3)}$$

$$Mg^{2+} + 2OH^- \rightarrow Mg(OH)_2 \text{ (4)}$$

Some ions from the metal surface that migrate to the solution, are known to form a protective film on the metal surface - Mg $(OH)_2$ formation is represented by equation 4. This Mg oxide layer is non-uniform and very porous, which is not sufficient to protect magnesium from further corrosion. In the presence of a high concentration of chlorides an $MgCl_2$ layer is formed instead of an $Mg(OH)_2$ layer, which is very soluble in water.[2] An example of microstructural features associated with corrosion of magnesium is depicted in **Figure 6.** It is possible to observe that localized corrosion started as irregular small pits and progressively

spread laterally, covering large areas, showing and confirming the high reactivity of magnesium.

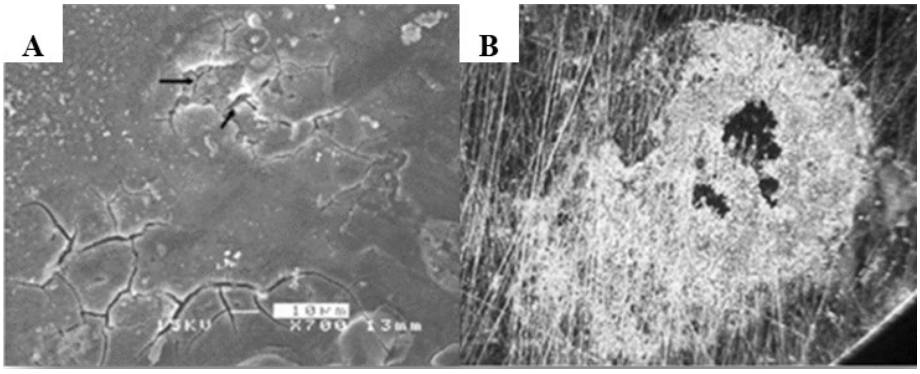

Figure 6 - Surface of magnesium after a corrosion test viewed by (A) SEM and (B) light microscopy. Adapted from [32].

Pure magnesium has a high corrosion rate at physiological pH (7.4-7.6), which can lead to the local formation of hydrogen gas (recall equation 1) and to an increase in pH and, consequently, cause cell necrosis. The rapid formation of hydrogen gas can also be a result of the rich chlorine environment in bodily fluids. Additionally, the high rate of gas formed can unsettle the mechanical properties of the implant, possibly affecting the healing process. [29]

An example of hydrogen gas accumulation is presented in **Figure 7**. It is possible to observe that a gas bubble was formed, subcutaneous, in guinea pigs after four weeks of magnesium alloy implantation. These gas pockets are due to a poor vascularization of the bone and insufficient mechanisms for removal of the hydrogen gas accumulated in excess near the implant, which may be harmful to human health.[29] This can cause inflammation and tissue necrosis [33] and, consequently, increase the time necessary for wounds to heal.[30] In addition, if large bubbles are formed and migrate to the circulatory system, they may cause a blockage of blood flow which, in turn, can lead to death.[30]

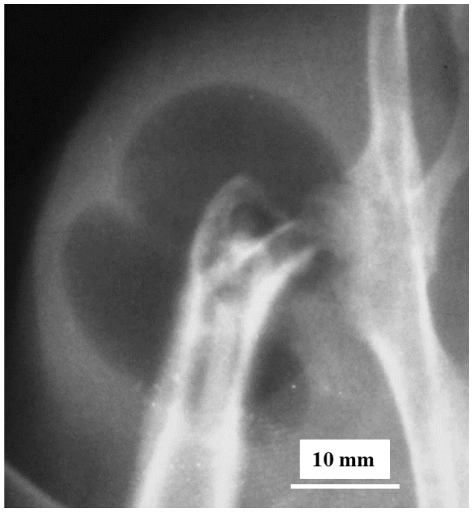

Figure 7 - Post-operative X-ray taken 4 weeks after a magnesium alloy implantation in which a subcutaneous gas bubbles is observed. Adapted from [25].

Nonetheless, at certain concentrations, the formed hydrogen gas can be stored in fatty tissues and quickly exchanged through the skin. A study by Song [34], states that for a hydrogen evolution rate of 0.01 mL/cm^2/day, the body can tolerate hydrogen gas formation without any consequences. Therefore, it is of great interest to achieve and maintain a corrosion rate that will allow the body to deal with the corrosion products of magnesium biodegradation. High corrosion rates can be influenced by different factors and mechanisms to improve the corrosion rate have been studied and placed into action in recent years.[30]

1.4. Methods for corrosion control/protection of magnesium alloys

The need to regulate the uncontrolled and fast corrosion of magnesium alloys led to the development of different strategies capable of overcoming these drawbacks: coating, alloying and surface treatments (**Figure 8**). Under each of these strategies there is a vast range of methodologies that can be combined or applied alone to control corrosion.[35]

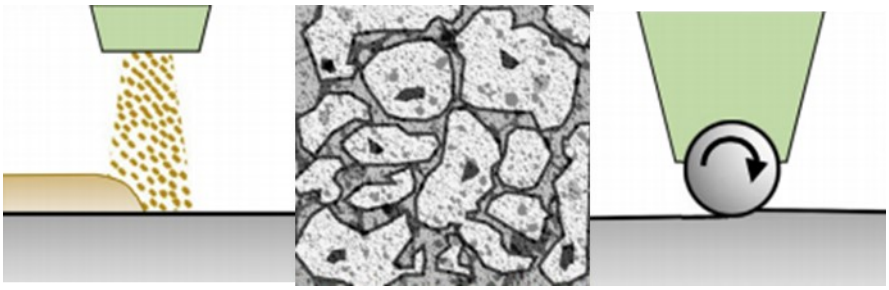

Figure 8 - From left to right: (left) coating, (middle) alloying and (right) surface treatments. Adapted from [35].

1.4.1. Alloying

Alloying elements in magnesium alloys are known to influence the properties of the alloy, improving their corrosion resistance, mechanical properties, biocompatibility and bioactivity. It has been reported that magnesium alloys such as AZ31, AZ91, WE43 and LAE44L have different corrosion rates, which are dependent on their composition and corresponding microstructure.[25] Therefore, element selection should be carefully weighed in, and taken into consideration characteristics such as element toxicity, corrosion behavior and the strengthening ability of the element.[36] The composition of some of the most common Mg alloys is presented in **Table 2**.

Table 2 - Alloying composition of common Mg alloys.

Designation	Alloying elements/Composition (wt%)	References
AZ31	Al- 2.5–3.5 % / Zn- 0.7–1.3 % / Mn- 0.2–1.0 % / Si- 0.05 % / Cu- 0.01 %	[37]
AZ91D	Al 9% / Zn 0.7% / Mn 0.3%	[38]
WE43	Rare earth elements: Neodymium- 71 % / Cerium- 8 % / Dysprosium- 8 % / Lanthanum- 6 %	[25]

The elements applied in the engineering of Mg alloys, can be divided into 5 groups from a nutrition and material science point of view. Elements can be grouped into impurities (Fe, Ni, Cu), well-known toxic elements (Pb, Cd, Th), nutrients found in humans (Ca, Cr, Mn, Zn, Sn, Si), nutrients found in plants and animals (Al, Bi, Li, Ag, Sr, Zr) and others (Sb, Gd, Y, Rare earth elements). Impurities induce a reduction in corrosion resistance due to a high difference in the electrochemical potential between the elements and the Mg alloys.[39]

Some rare earth elements as well as elements such as calcium, zinc and manganese are reported to delay biodegradation and are not toxic to the human organism.[40] Some of the elements used in alloying and their characteristics can be observed in **Figure 9**.

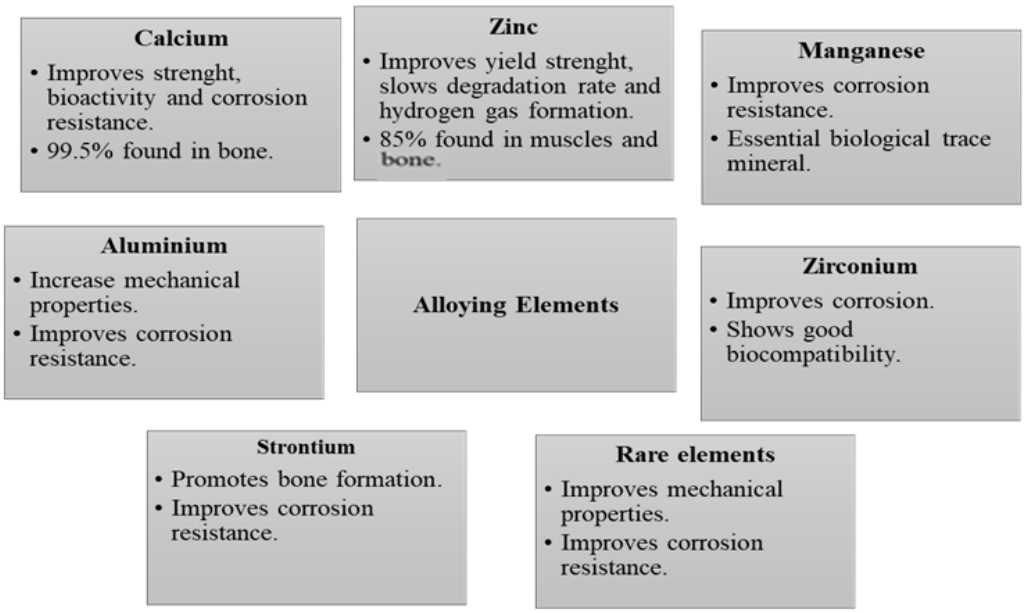

Figure 9 - Known elements used and their promising potential as alloying elements.[29] [39]–[41]

Calcium (Ca) is an abundant mineral mainly present in bone and teeth known to promote bone healing and often added to improve corrosion resistance. It also increases the strength and elongation rate of the magnesium alloys. Additionally, an excess amount of calcium can cause a reduction in the corrosion rate.[42] Calcium is also one of the elements in hydroxyapatite (a mineral that makes the bone more stable and rigid). The release of Ca and Mg from Mg-Ca alloys, can potentially improve bone healing, transforming these alloys into potential osteoconductive implants.[43] One example is that of the Mg-0.8Ca alloy which, when tested *in vitro* immersed in HBSS (Hank's balanced salt solution), showed to be biocompatible and bioactive, demonstrating the potential of this type of binary alloys as biodegradable implants.[43]

In addition to calcium, zinc is often used as an alloying element for magnesium alloys. It is of great importance to hundreds of biological enzymes and transcription factors. It is also quickly absorbable by biological functions within the cell. Magnesium alloys with zinc have also shown to be less prone to hydrogen gas formation.[29]

Manganese is an essential biological trace mineral in many roles within cellular systems, specifically as different co-factors for metalloenzymes (e.g. DNA and RNA polymerases). It is known to reduce the effects of the impurities present in magnesium (naturally present or from casting/refining processes) improving the corrosion resistance of magnesium and its alloys.[29]

Further improvement of the corrosion behaviour of Mg and Mg alloys may also be achieved by surface modification.[34]

1.4.2. Surface modifications: surface treatments and coatings

In order to overcome the high corrosion rate of magnesium and its alloys in the human body and to obtain the desired rate of corrosion, surface modifications have been explored in recent years.[2][5][45] Surface modification of a magnesium alloy, for biomedical implant applications, can provide a barrier against the surrounding environment thus having a significant role in the degradation rate of the implant.[31] These modifications can be achieved in terms of surface coating, surface treatment or a mixed treatment of the previous two. A surface treatment consists on the modification of the composition, microstructure (or both) of the material's surface whereas a surface coating corresponds to the addition of a layer of a material to the alloy's surface.[5]

For a coating to be considered effective it must be uniform, free from scratches, pits and cracks as well as adherent.[31] However, the non-uniform ($Mg(OH)_2$) layer present at the surface of the Mg alloy will have a detrimental effect on the coating's adherence to the metal surface and on the formation of an uniform protective layer, affecting its overall performance. Therefore, a surface pre-treatment is an essential factor to achieve an effective coating.[31]

Coatings can be achieved by different methods of preparation such as mechanical, physical, chemical biological, or biomimetic.[45]

Surface treatments can be achieved mechanically for example by friction or attrition; biologically by bio-mineralization and molecular recognition; physically by ion implant, and diffusion treatment; and chemically by thermal treatment and, for example, micro-arc oxidation.[45]

Surface coatings can also be divided into two types of coatings according to the type of formation. Conversion coatings are grown *in situ* (directly on the surface of the material) and are formed by specific reactions between the base material (metal) and the environment.[44] Typically, the metallic substrate surfaces are converted, through chemical or electrochemical processes. The produced layers are usually inorganic and show a ceramic-like character (e.g. hydroxyapatite).[44] Deposited coatings consist mostly of polymeric-based materials.[44]

In practice, it is quite common to combine different types of surface treatments and coatings to obtain the best results in different areas, from aeronautical to biomedical fields. For example, before any type of coating application the metallic substrates tend to be mechanically polished and chemically clean, followed by the growth or application of a thin inorganic or

hybrid-like layer with the main role of improving adhesion of the substrate to the organic coating applied in the final stage.[2][5][45]

In the following sections additional information regarding to the coatings used in this work is presented.

1.4.2.1. Conversion coatings

Several techniques can be used to obtain conversion coatings. One of the most promising inorganic-based biomimetic coating, due to its chemical similarity to the mineral phase of bone, is a hydroxyapatite coating.[46]

The calcium phosphate (CaP) family is composed of different crystal phases formed in different CaP molar ratios. Since two of the main minerals composition of bone is Ca and P, these CaP coatings are seen as very promising materials in the orthopedical field. CaP is non-toxic, presents a controlled degradation and is very biocompatible and bioactive.[47] One of the major properties is the ability to form a close physicochemical bond between the implant and bone (osteointegration).[47]

Hydroxyapatite ($Ca_{10}(PO_4)_6(OH_2)$) is one of the different crystal phases from the calcium phosphates family.[46] It is a bioactive material that promotes bone cell adhesion and proliferation and shows good biocompatibility. Other minerals like tricalcium phosphate (TCP) also contribute to bone formation and higher biocompatibility.[4]

HAp seems to be the most promising of the crystal phases to be used as a coating material in orthopedics. With a Ca/P ratio of 1.67, HAp is the most stable phase, the dominant mineral in bone has a slow degradation rate and is osteoconductive (but not osteoinductive).[48]–[50]

The corrosion resistance and controlled degradation of HAp- coated Mg alloys have been already acknowledged in different studies, such as HAp coatings on AZ31 and AZ39. These *in vitro* tests, performed in a SBF solution, showed an increased corrosion resistance behavior.[38] [51] [52] Studies on biocompatibility are scarce, however the ones reported in the literature, such as the cytotoxicity and hemolysis assessment of a HAp coated- Mg-Zn-Ca-Zr alloy, have shown great potential. In this particular study, cytotoxicity was evaluated with L929 fibroblasts and results similar to the negative control were obtained being, therefore, considered non-cytotoxic. The hemolysis rate obtained met the requirements necessary to be used as implant materials (<5%).[53]

HAp is a promising material, however, there are still some challenges to overcome, one of which is its brittleness which limits their use as biomaterials for load-bearing applications.

Nevertheless, by combining HAp with polymeric coatings this can potentially be overcome.[46] [47]

1.4.2.2. Deposited coatings

Deposited coatings typically consist of organic (polymer) materials although some work has been reported on inorganic, metal and inorganic/organic coatings. However, in the scope of this work, we will focus on organic coatings, specifically.[2]

Organic-based coatings offer protection against corrosion and other functions such as drug delivery and the ability to be functionalized with organic biomolecules. Organic coatings can include a variety of different processes that use organic polymers and are achieved, for example, by dipping the metal in an organic (polymer) solution.[2][44]

Degradable polymers have been applied in various areas including biomedical applications.[2] Polymeric coatings based on polymers such as polylactic-co-glycolic acid (PLGA), polylactic acid (PLA), polycaprolactone (PCL) and polyetherimide (PEI) possess good biocompatibility, making them a good choice as coatings for magnesium and its alloys.[2]

Polyetherimide, as a biomaterial, has shown to be biocompatible, non-cytotoxic and non-hemotoxic, stimulating fibroblast formation in vivo, cell spreading and growth.[54] PEI has been applied as coating due to its mechanical properties being compatible with those of magnesium and its alloys.[55] It is a promising candidate for the corrosion protection of magnesium and its alloys due to its hydrophobic nature, thermal and mechanical stability.[56] Studies have also shown that the presence of PEI coatings enhanced resistance to corrosion.[55] Reports on the use of PEI as a coating for the corrosion protection of magnesium alloys are few, however they revealed promising results, encouraging the use of this polymer in protective coatings of Mg alloys for orthopedic applications.[57]

1.4.3. Active species/corrosion inhibitors

Among the various methods to avoid or prevent degradation of a metal surface by corrosion, the most useful and best known is the use of corrosion inhibitors.[58] Inhibitors are chemicals that react with a metallic surface, or the environment, to which the surface is exposed, giving it a certain level of protection, hence minimizing corrosion.[58] [59] They can be added directly to the corroding media in contact with the metal or incorporated into the protective coating to render active protection and when electrolyte penetrates the coating and reach the metal surface. There are few reports on corrosion inhibitors for magnesium and its alloys such as F^- salts, $Cr_2O_7^{2-}$ salts and 8-hydroxyquinoline (8HQ). However, F^- and $Cr_2O_7^{2-}$ are highly polluting as well as toxic and therefore, alternatives must be taken into

consideration.[59] As an example, the use of 8-hydroxyquinoline (8HQ) has been reported and its inhibition effect was tested with AZ91D magnesium alloy. Results showed that the presence of 8HQ enhanced the corrosion protection of the studied magnesium alloy.[60] In addition to corrosion-inhibiting species, other active species capable of enhancing and promoting bone healing may also be introduced into coatings to work as a drug delivery system.[62][63]

1.5. Enhancing bone healing by drug delivery

Some pathologies, inherent to certain patients, can delay and sometimes impair the healing process of a fracture. Different active species, when in a targeted delivery system, can act as adjuvant therapeutic agents, maximizing the healing process and promoting tissue regeneration. Growth factors, antibiotics, hormones, non-steroidal anti-inflammatory drugs, among others, are some of the active species that can help the healing process. Natural and synthetic polymers, such as PLGA, PLA, PCL, are known carriers in drug delivery systems.[62][63]

Gelatin is a natural polymer widely studied and applied in pharmaceuticals and medical applications, as a drug delivery system for different types of active species.[63] It is also considered a GRAS (Generally Regarded as Safe) material, by the American FDA (Food and Drugs Agency).[64]

Gelatin is derived from collagen and due to its high availability is very affordable. It is also highly biocompatible, biodegradable (in physiological environments) and has low antigenicity activity (metabolic products resulting from degradation are harmless). The versatility of gelatin has led to great interest in it as a drug delivery vehicle, since gelatin can be chemically modified to maximize loading efficiency, by modifying the isoelectric point of gelatin during its synthesis process. The release profile can also be adapted by varying the molecular weight of the gelatin or the amount of the cross-linking material.[63]–[65]

Gelatin can be modified into a different types of carriers: hydrogels, fibers and microparticles/nanoparticles, among others.[65] Both microparticles and nanoparticles have been extensively used to encapsulate bioactive molecules. Microparticles can be used as carriers for large bioactive molecules due to their large surface area. Nanoparticles are more suited for targeted drug delivery in the body and have higher intercellular absorption than microparticles.[65] Gelatin loaded with active species, can be used to coat different implants with other natural or synthetic polymers.[64] **Figure 10** depicts a gelatin particle.

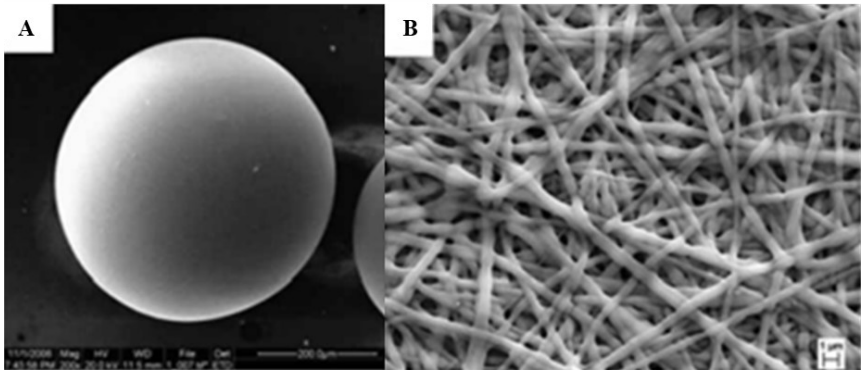

Figure 10 - Scanning electron microscopic images of (A) gelatin particle, with a magnification of x3000 and (B) a crosslinked gelatin map, crosslinked with 0.1 % w/v genipin. Adapted from [65].

The main drawback of gelatin is the high ability to absorb water, which leads to a fast release of water-soluble compounds. However, this can be overcome by controlling the water uptake, modifying the gelatin source, molecular weight, or the crosslinking degree.[64][65]

Calcium carbonate ($CaCO_3$) is an abundant inorganic, non-toxic, chemically stable and biocompatible biomaterial, widely used in orthopedic, drug delivery and biomedical applications.[66][67]

$CaCO_3$ particles can be synthesized through low-cost and facile methods and can precipitate in 3 different polymorphs. Vaterite, calcite and aragonite are $CaCO_3$ polymorphs with hexagonal, rhombohedral and orthorhombic crystalline structures, respectively.[66] These 3 different polymorphs are presented in **Figure 11**.

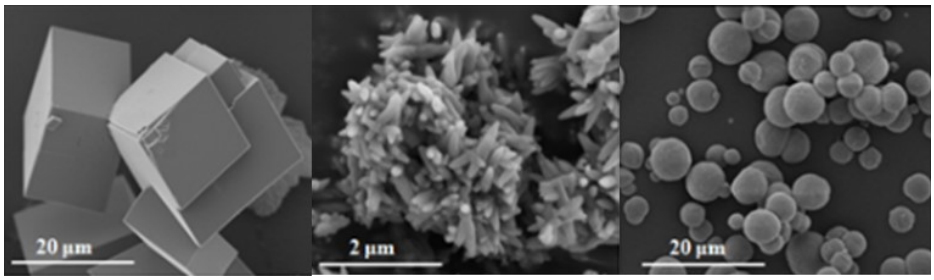

Figure 11 - From left to right, typical shapes of calcite, aragonite and vaterite. Adapted from [68].

Vaterite, from all the polymorphs, is the one with the most potential to be used as a drug delivery carrier due to its low thermodynamic stability, high solubility and spherical shape.[68]

All the above techniques and additives, to improve biocompatibility and achieve controlled biodegradation of magnesium alloys, make these alloys a promising medical device. However, it's of extreme importance to guarantee the biological compatibility with the human body, therefore, a biocompatibility evaluation of the device potential is required.

1.6. Medical devices testing for biocompatibility

Assessment of the biocompatibility of a medical device is mandatory when no previous data on the toxicity of its components is available. Biocompatibility studies may comprise both *in vitro* and *in vivo* tests. Medical devices can be divided into categories, according to ISO 10993-1: 2018, in nature and duration of body contact, as presented in **Table 3**.

Table 3 - Biological evaluation tests considered in the context of a medical device testing, adapted from [69].

Medical device categorization by			Biological Effect							
Nature of body contact		Contact duration	Cytotoxicity	Sensitization	Irritation or intracutaneous reactivity	Systemic toxicity(accute)	Subchronic toxicity (subacute toxicity)	Genotoxicity	Implantation	Hemocompatibility
Category	Contact	A- limited (<24 h) B- prolonged (>24 h to 30 d) C-permanente (>30 d)								
Surface device	Skin	A	x	x	x					
		B	x	x	x					
		C	x	x	x					
	Mucosal membrane	A	x	x	x					
		B	x	x	x					
		C	x	x	x		x	x		
	Breached or compromised surface	A	x	x	x					
		B	x	x	x					
		C	x	x	x		x	x		
External Communicating device	Blloth path,indirect	A	x	x	x	x				x
		B	x	x	x	x				x
		C	x	x		x	x	x		x
	Tissue /Bone/ dentin	A	x	x	x					
		B	x	x	x	x	x	x	x	
		C	x	x	x	x	x	x	x	
	Circulating blood	A	x	x	x	x				x
		B	x	x	x	x	x	x	x	x
		C	x	x	x	x	x	x	x	x
Implant device	Tissue/Bone	A	x	x	x					
		B	x	x	x	x	x	x	x	
		C	x	x	x	x	x	x	x	
	Blood	A	x	x	x	x	x		x	x
		B	x	x	x	x	x	x	x	x
		C	x	x	x	x	x	x	x	x

Table 3 depicts the different sets of tests that might be necessary for the biocompatibility testing of medical devices according to ISO 10993-1:2018. Depending on the nature and duration of body contact, different tests are required by the regulatory bodies for the biological safety evaluation of medical devices.[69]

As shown in **Table 3**, *in vitro* cytotoxicity testing is mandatory for medical device testing regardless of the nature and duration of the contact. On the other hand, hemocompatibility assessment is only necessary when a close contact of the device with blood is expected to occur. According to the obtained results, it might be necessary to rethink the device by performing changes to its composition, excluding the hazardous components.[69]

1.6.1. Cytotoxicity

Cytotoxicity is a state induced by a toxic agent that can cause cell damage (e.g. cell death, changes in the cellular membrane permeability, enzymatic inhibition, etc.). Hence, an Mg alloy would be considered toxic, if the release of its elements would induce cell damage or death. This could happen directly or through the suppression of key metabolic pathways.[70]

ISO 10993-5 [71] standard provides guidance on how to perform *in vitro* cytotoxicity testing of medical devices. The most adequate method to employ is selected based on the nature of the sample, the potential site of use and the character of its use. Mouse L929 fibroblasts are one of the recommended and the most frequently used cell lines for medical devices *in vitro* cytotoxicity testing. Thus, medical devices can be tested using direct or indirect methods.[70] In the direct method, cells are in direct contact with the material and tested for cytotoxicity following exposure. In the indirect method, an extract of the material is prepared, usually in serum-free cell culture medium. ISO10993-12 [72] indicates the most suitable vehicles and conditions extractions to be followed, according to the purpose of the test, nature and application of the final product. Extraction can be influenced by different factors such as time, temperature, surface area-to-volume ratio, among others.[72]

In **Table 4** different cytotoxicity endpoints, that can be assessed for the biological evaluation of medical devices, are presented.

Table 4 - Possible endpoints and the respective methods or assays used to determine cytotoxicity.[70]

Parameter	Method/Assay
Cell morphology	Phase-contrast microscopy.
Cell membrane integrity	Lactate dehydrogenase assay. Propidium iodide assay.
Celular metabolic activity	Fluorescein diacetate assay. Reduction of tetrazolium salts assay (MTS, MTT, WST-1). Resazurin-based assays (Alamar Blue, PrestoBlue).

Where MTT represents 3-(4,5-dimethylthiazol-2-yl)-2,5-diphenyltetrazoliumbromide and MTS represents 3-(4,5-dimethylthiazol-2-yl)-5-(3-carboxymethoxyphenyl) - 2-(4-sulfophenyl)-2H-tetrazolium

Phase-contrast microscopy, a qualitative method, allows detailed observation of cell morphology, which might be useful to detect potential alterations in the cellular aspect after exposure. Changes in cell viability can be evaluated by the fluorescein diacetate (FDA) assay/propidium iodide (PI) assay. This test allows the differentiation of live cells from dead cells. FDA is a non-fluorescent molecule, which is hydrolyzed to fluorescent fluorescein in live cells. PI is a red-fluorescent nuclear and chromosome counterstain that binds to DNA by intercalating between the bases with little or no sequence preference. It is not membrane-permeant, allowing detection of dead cells in a population. Plasma membrane integrity can be evaluated through the Lactate Dehydrogenase (LDH) release assay. LDH is a soluble enzyme, present in the cytosol, that is released into the extracellular medium when the plasma membrane is damaged and therefore can be used as an indicator of cell membrane integrity.[73]

To assess effects upon the cellular metabolic activity, different assays can be carried out. Tetrazolium salts compounds can be converted by viable cells to the soluble and colored formazan which, in turn, will cause a significant increase in color intensity, that can be easily quantified by measuring its absorbance at 490-500 nm. The most used assays include MTT, MTS and WST. These tests use spectrophotometric quantification to measure proliferation, viability, growth and chemosensitivity in cell populations. Resazurin (7-hydroxy-3H-phenoxazin-3-one-10-oxide) assays are also based on the ability of viable cells to reduce resazurin to resorufin, a pink and fluorescent precipitate, that can be measured colorimetrically or fluorescently. Common resazurin reduction assays include Alamar Blue and PrestoBlue.[74]

1.6.2. Hemocompatibility

When a medical device is introduced in the human body and contacts directly with blood, many reactions might take place. Hemocompatibility of blood-contacting medical devices must be assessed to guarantee that blood and/or its components are not adversely affected.[75]

Blood is composed of elements such as the red blood cells, leukocytes and platelets in an extracellular matrix, the plasma. Blood possesses a large variety of proteins, with different functions and at different concentrations. These proteins are of the outmost importance in the biomaterial-blood interaction.[76] Albumin, immunoglobulins and fibrinogen represent 50% of the proteins present in the plasma. These proteins, as well as others, are responsible for some of the adverse reactions that might occur when a foreign element comes into contact with them. For example, fibrinogen has the main role in the process of thrombosis, and proteins like fibronectin and von Willebrand factor have shown the ability to mediate platelet adhesion to the biomaterials. Prior to contact with host cells, a layer of plasma proteins will get adsorbed at the surface of the device, when it contacts with blood. This layer will be responsible for the interaction between the blood and material, defining what type of reactions will occur. It is the interaction between the adsorbed proteins and inflammatory cell populations that mostly contributes to the recognition of the implantable biomaterials by the organism.[76]

It is also important to understand how blood contact with the material is influenced by the material's surface properties. These properties must be taken into consideration when assessing the hemocompatibility of the metal alloys, as they play a role in cell and platelet adhesion.[77]

According to ISO10993-4 [75], the recommended tests can be divided into categories as presented in **Figure 12**.

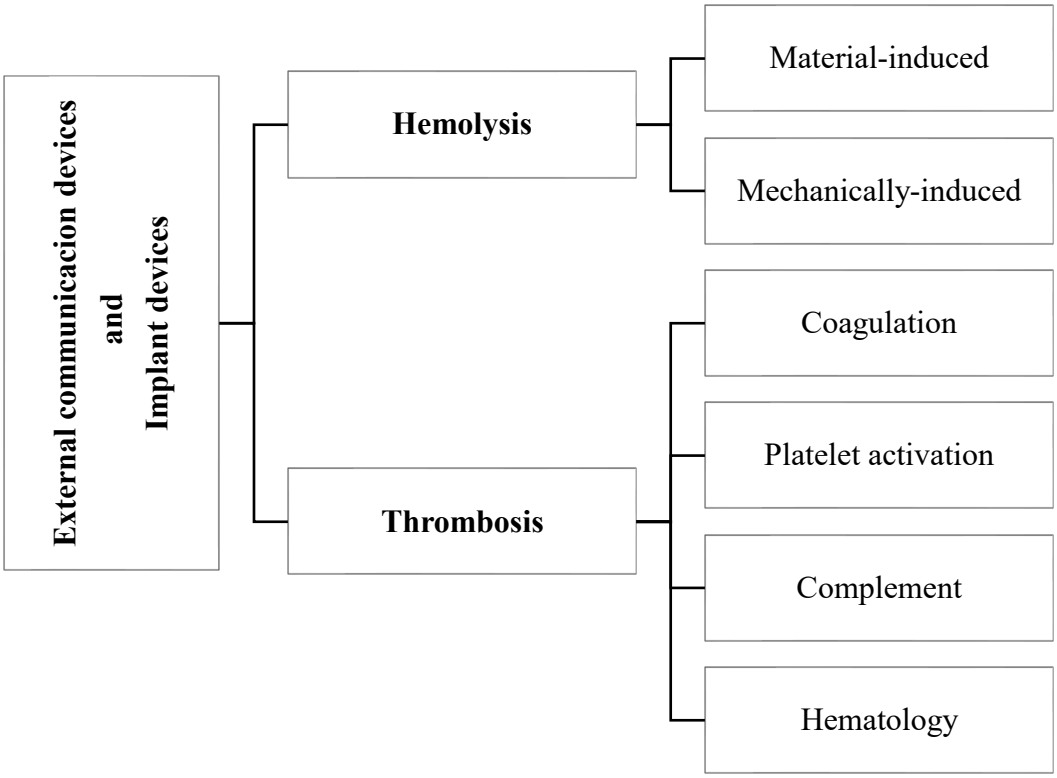

Figure 12 - *In vitro* test categories to consider for external communication devices and implant devices.[75]

Figure 12 presents the *in vitro* tests recommended for the hemocompatibility evaluation of external communicating implant devices. Usually, the *in vivo* method is preferred when testing for thrombosis. Nevertheless, the combination of different tests such as coagulation, platelets, hematology and complement system activation, can be used as an alternative. If reactions such as thrombus formation, hemolysis, platelets and complement system activation occur, the material might not be considered safe.[75]

Aspects such as the anticoagulant type and amount, test sample preparation and others should be taken into consideration as they might influence *in vitro* hemocompatibility tests. Moreover, *in vitro* testing tests should be performed within 4 hours after blood drawing to minimize changes in blood properties over time.[75]

1.6.2.1. Hemolysis

Hemolysis occurs when the membrane of the erythrocytes is partially or totally destroyed and their main protein, hemoglobin (Hb) is released to the plasma, after blood-material interaction. The material interacts with blood through the adsorption of plasma proteins which adsorb in seconds.[78]

Hemolysis screening is considered of great importance, since an abnormal value of plasma-free Hb may cause serious health problems. Hemolysis may occur due to the direct contact of red blood cells (RBCs) with the material or by exposure to the chemicals released

from the material. There are different methodologies to estimate the Hb content of a sample such as the classical cyanmethemoglobin method, the iron method, direct optical and added chemical techniques, among others.[75]The cyanmethemoglobin method is based on the oxidation of Hb and subsequent formation of hemiglobincyanide (HiCN), which has a broad absorption maximum at 540 nm. This method has the advantage of using a primary reference standard, HiCN, that is prepared from erythrocytes lysates. Accordingly, this method allows a comparison between the sample absorbance and the HiCN standard solution while minimizing plasma spectral interference.[75]

Another alternative to the cyanmethemoglobin method is the iron method. This method determines Hb iron concentration in solution. After ashing or acid treatment, iron is separated from Hb. The iron is measured photometrically after being complexed with a reagent in order to develop color.[75]

1.6.2.2 Thrombosis

A device/material might have a thrombogenic potential that refers to the tendency to produce a thrombus once in contact with blood. A thrombus, or clot, results from blood coagulation and is formed by aggregated platelets, erythrocytes and fibrin.[79]

Fibrin is the main component of a thrombus which is formed by the action of thrombin on fibrinogen through a cascade of events. To assess coagulation, important proteins in the coagulation cascade, such as thrombin and fibrin are usually measured and quantified by Enzyme-Linked Immunosorbent Assay (ELISA).[78]

Platelets also participate in the thrombosis process. They are present in the blood as cellular bodies, with no nucleus. Materials might show a tendency to promote platelet adhesion to its surface.[76] Upon adhesion to the material surface, platelets will release factors to stimulate further platelet activation that increases local platelet aggregation leading to the formation of a platelet thrombus, as depicted in **Figure 13.**

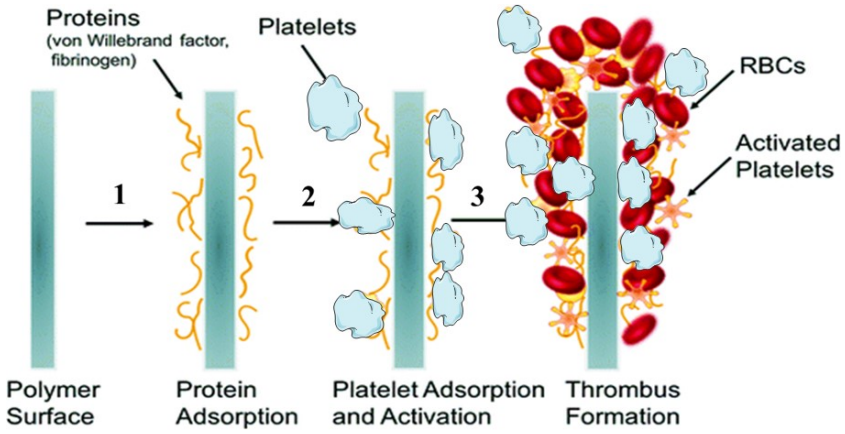

Figure 13 - Illustration of thrombus formation induced by the interaction between blood and a polymer surface. Adapted from [80].

Platelet adhesion to material's surface, under certain conditions of flow and pressure, can be estimated based on the loss of whole blood platelet upon exposure to the material. Alternatively, the number of adherent platelets, present on the material's surface, can be counted using light or scanning electron microscopy (SEM).[78]

In hematology, the complete blood count is a vital test that can quickly determine the concentration of different cell populations in the blood. It quantifies the number and proportion of white cells and red blood cells in the organism.[75]

The complement system is a part of the immune system. It contains more than 30 plasma proteins acting as a defender by mediating specific antibody mechanisms. It is present in blood plasma and works as a biochemical cascade, that will complement the antibodies against pathogens in the body and can also be activated by the surface of certain materials outsiders to the body, as the magnesium alloys.[81] Among all the proteins of the complement system, C3 is one of the most used and considered a good indicator of complement system activation, since C3 is an ubiquitous fragment amplified during activation. It can be measured by ELISA assays.[75]

The complement system can be divided into three activation pathways: the classical complement pathway, the alternative complement pathway and the mannose-binding lectin pathway. The alternative pathway has been known to be the most reactive to the presence of foreign materials.[81]

1.7. Cytotoxic and hemotoxic effects of magnesium alloys

In what concerns biocompatibility testing and comprehension on Mg alloys, reports in the literature are more extensive on the cytotoxic potential than on the hemotoxic one.

Myrissa and collaborators observed that pre-osteoblasts seeded onto Mg, Mg2Ag and Mg10Gd discs distributed homogeneously along the surface of the alloys and no significant changes in cell viability were detected within 13 days post-seeding compared to control cells, as seen in **Figure 14.**[82]

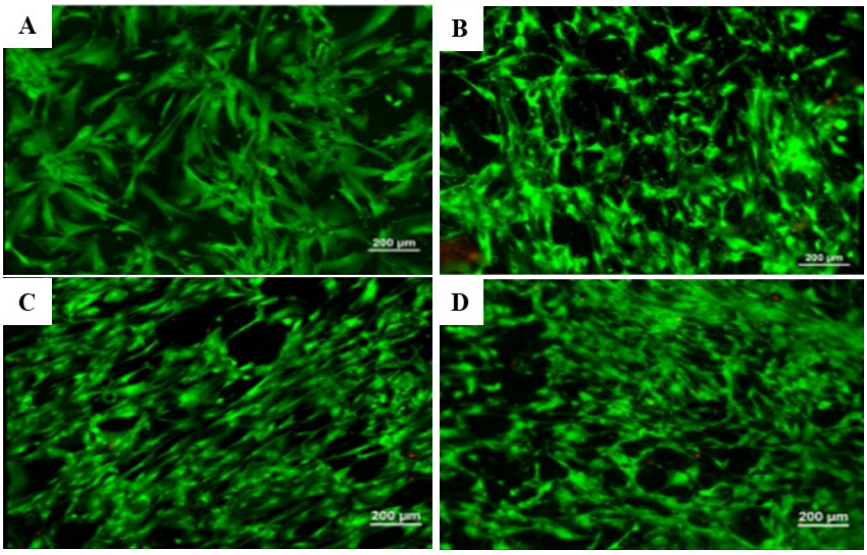

Figure 14 - Fluorescent microscope images of pre-osteoblastic cells after 13 days of proliferation in a Mg alloy of (A) control (B) Pure Mg (C) Mg2Ag and (D) Mg10Gd. Live cells in green, and dead cells in red, 20×magnification.Adapted from [82].

AZ31 alloy with ion N^+ implantation was also tested, indirectly, by MTT assay on NIH-3T3 mouse fibroblasts. After 2 days of culture, low levels of cytotoxic effects were found, suggesting that the alloy can be used as a biological material.[83]

Studies in literature, suggest that surface coating might influence the cytotoxicity of Mg alloys. ZK60 Mg alloy, coated with strontium doped calcium phosphate, showed good biocompatibility in MC3T3-E1 cells compared to the unmodified magnesium alloy, as assessed by adhesion, proliferation and hemolysis.[84] More complex systems have also been tested, such as an Mg alloy with a multifunctional coating constituted by polydopamine, dicalcium phosphate dehydrate and collagen. Cytotoxicity was evaluated on murine calvarial pre-osteoblasts cells (MC3T3-E1) by alkaline phosphatase assay (ALP), live/dead assay and cellular adhesion and morphology imaging. This system exhibited good cytocompatibility by providing an interface for cell adhesion and growth.[85] Another system, an AZ91 magnesium alloy coated with calcium phosphate and antimicrobial peptides, loaded on the surface, was evaluated for cell proliferation on rat bone marrow mesenchymal stem cells (rBMMSCs) by the MTT assay. After cultured for 20 days, an ALP test was also performed. Overall, results

showed good biocompatibility by promoting ALP activity, and also by promoting bone repair.[86]

Evidence reported in literature, suggests that the alloying elements may also account for the in vitro toxicity of Mg alloys. Gu et al. investigated the cytotoxicity and hemotoxicity of binary Mg–1X (wt.%) alloys synthesized with 9 alloying elements (Al, Ag, In, Mn, Si, Sn, Y, Zn and Zr) in fibroblasts (L-929 and NIH3T3 cells) and osteoblasts (MC3T3-E1 cells). The obtained data showed that Mg–1Al, Mg–1Sn and Mg–1Zn alloy extracts did not induce significant changes in fibroblast cell viability whereas extracts of Mg–1Al, Mg–1Si, Mg–1Sn, Mg–1Y, Mg–1Zn and Mg–1Zr alloys were not cytotoxicity to osteoblasts. Hemolysis assays were also performed and the obtained results showed that Mg-1ln, Mg-1Mn, Mg-1Si and Mg-1Y alloys caused less than 5 % hemolysis.[39] Moreover, a Zn-1-Mg0.1Sr alloy showed a reduced rate of hemolysis, while Zn-1-Mg0.5Sr alloy showed no signs of thrombogenicity.[87]

The larger part of the scarce information available on Mg alloys hemocompatibility is on different alloying elements. When it comes to more complex systems the majority of the literature only reports cytotoxic results and no information on the potential hemotoxic effects is found. Nevertheless, the few existing studies on different alloying elements, for magnesium alloys, offer good perspectives about the hemocompatibility of this alloy.

1.8. Current clinical orthopedic applications of biocompatible magnesium alloys implants in humans

Since the beginning of the last decade that Mg alloys have been intensively studied due to their promising properties in the clinical field. Besides *in vitro* assessment, *in vivo* preclinical studies have been performed on Mg and its alloys to assure their safety and effectiveness before clinical trials.[88]

Currently, there is only one Mg alloy available in the market for clinical use, a Mg compression screw (MAGNEZIX® CS, Syntellix AG, Hanover, Germany) that is composed of magnesium, zirconium, yttrium and other rare earth metal (MgYREZr).[89] This Mg implant obtained CE certification in 2013 and entered the European market in 2014, having over 4000 implants sold.[90] This Mg-based screw has been successfully applied in orthopedic surgery, showing good results compared to conventional metallic implants. In this regard, a prospective, randomized, controlled clinical pilot study compared Mg-based MgYREZr *vs* conventional Ti-based screws in terms of fixation during chevron osteotomy in patients (n=25) with a mild hallux valgus.[91] After 1-year postoperative, both functional and radiological outcomes

showed significant improvements in both groups, yet radiological improvements were significantly better in the group of patients with the Ti-based screws.

The biodegradable Magnezix® CS screw has been also been successfully used for the fixation of fractures of the condylar head of the mandible.[92] A three-month follow-up study in five patients, implanted with the Mg-based screws, demonstrated that no swelling associated with the hydrogen gas formation or any other complications from the degradation of the alloy were observed. The implant also showed good biomechanical stability, providing a better alternative to the typical Ti screws.[92] **Figure 15** presents different Mg-based screws available in the market (A) or under clinical trial (B and C). Besides the approved screw in the market, only other two biodegradable metallic screws have been approved for clinical trials.[12]

Figure 15 - From left to right, the MAGNEZIX, RESOMETÒ and pure magnesium screws [12], [93].

RESOMETÒ (K-MET), an Mg-Ca-Zn alloy screw, was approved for a clinical trial by the KFDA (Korea Food and Drug Administration). This screw was tested in the treatment of hand fractures in 53 patients. The results showed that after 12 months, the implant was substituted by new bone, demonstrating the potential of the biodegradable screws.[12], [94] A pure magnesium screw was approved to be tested in a 48 patient clinical trial in China for the treatment of osteonecrosis of the femoral head. The results showed bone formation, no adverse effects, that could have been induced by the products of degradation as well as no observable formation of gas, suggesting a promising bone screw fixation.[93]

Some studies on the application of Mg alloys as orthopedic implants are summarized in **Table 5**.

Table 5- Clinical studies on the orthopedic application of magnesium alloys.

Reference	Type of implants	Implantation site	Follow-up
2013[94]	Mg-5wt%Ca-1wt%Zn alloy Screws	53 hand and wrist fractures	Formation of bio mimicking calcification matrix at the degrading interface. After 1-year, the formation of new bone.
2016[93]	Mg screws with purity of 99.99 wt.%	Fixation of vascularized bone graft in osteonecrosis of the femoral head	Tissue necrosis and abnormal blood chemistry around the screw were not found post-implantation. Greater bone formation around the screw after 12 months implantation.
2018[95]	High pure Mg screws	Avascular necrosis of the femoral head	Effective after a 2 years follow-up, no significant progressive necrosis of the femoral head was found. Mg screw gradually degraded in the human body.
2019[96]	MAGNEZIX CS	Distal chevron osteotomy in hallux valgus. (n=16)	No superficial or deep infection developed in any patient. Implant removal was avoided.

Chapter 2: Materials and Methods

2.1. Materials

Mg1Ca alloys were cast at Helmholtz-Zentrum Geestacht (HZG), Geestacht, Germany. Mg1Ca alloys were polished, prior to any pre-treatment, with a silicon (Si) paper (from 400 to 2500 grit), rinsed with isopropanol, dried in a stream of warm air and kept stored until further use.

Reagents used to prepare a hydroxyapatite layer, namely ethylenediaminetetraacetic acid calcium disodium salt hydrate (Ca-EDTA: $C_{10}H_{12}N_2O_8Na_2Ca$), potassium dihydrogen phosphate (KH_2PO_4) and sodium hydroxide (NaOH), used to adjust the pH, were obtained from SIGMA-ALDRICH.

The coating was prepared by preparing a polymer solution, using polyetherimide (PEI) ULTEM 1000® kindly provided by HZG and dichloromethane (DCM), CH_2Cl_2, from SIGMA ALDRICH. The coating also included gelatin microcapsules and calcium carbonate particles. To synthesize gelatin microcapsules, gelatin from bovine skin and D-glucose were obtained from SIGMA, anhydrous calcium chloride ($CaCl_2$) obtained from CARLO ERBA REAGENT, Span® 85 ($C_{60}H_{108}O_8$) from SIGMA-ALDRICH and sunflower oil (commercially available). For the calcium carbonate particles synthesis, anhydrous calcium chloride ($CaCl_2$,) and sodium carbonate (Na_2CO_3) from ALFA AESAR were used.

In cytotoxicity assays, the fibroblast cell line L929 used was obtained from the American Type of culture collection (ATCC; CCL1). Cell mediums used to maintain cells and for extract preparations were the Minimum Essential Medium Eagle (MEM) and Dulbecco's Modified Eagle Medium (DMEM). Both mediums and Trypsin-EDTA (0.25% solution) were obtained from SIGMA ALDRICH. MEM used was supplemented with 4 mM L-glutamine, 100 units/mL of penicillin, 100 µg/mL of streptomycin and 10% of heat-inactivated fetal bovine serum (FBS). DMEM contains 4 mM L-glutamine, 100 units/mL of penicillin and 100 µg/mL of streptomycin. LDH and WST-1 kits were obtained from Roche Applied Sciences.

For hemocompatibility assays, to detect human C3a, an ELISA kit was obtained from Invitrogen, Thermo Fisher Scientific.

2.2. Methods

This work was performed in a collaboration with the Institute for Public Health of the University of Porto (ISPUP). The multilayer systems were synthetized and all tests concerning the multilayer system characterization were executed in the University of Aveiro. The biocompatibility assays were conducted in ISPUP.

2.2.1. Preparation and characterization of the multilayer coating

2.2.1.1. HAp pre-treatment

Mg1Ca alloys were immersed in a mixture of 250 mM of Ca-EDTA and 250 mM of KH_2PO_4 solution. The pH of the prepared solution was then adjusted to 8.9 using a NaOH solution. Mg1Ca alloys were kept in the mixture, for a period of 6 h, in a water bath at 90ºC. Mg1Ca alloys were then removed, washed with deionized water, dried with a warm stream of air and kept, until further use, in a desiccator. An illustration of the experimental procedure is presented in **Figure 16**.

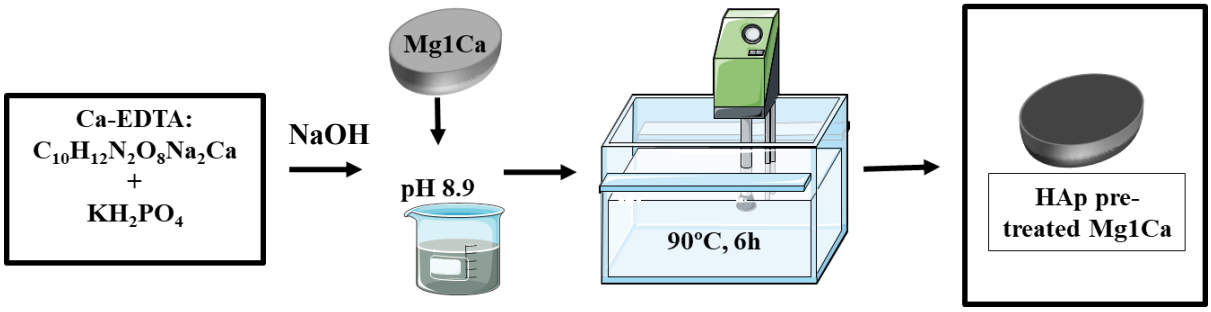

Figure 16 - Illustration of Mg1Ca pre-treatment with hydroxyapatite.

2.2.1.2. Coating preparation

2.2.1.2.1. Polymer solution

A solution of PEI 10 wt% was prepared, by dissolving an appropriate amount of PEI in dichloromethane, to obtain the polymer solution. This solution was kept under stirring until complete dissolution was achieved.

2.2.1.2.2. Synthesis of gelatin microcapsules

Gelatin microcapsules were synthesized by a thermal gelation method, following a published procedure.[97] A 20% w/v aqueous gelatin solution was prepared, by adding 4 g of gelatin to 20 mL of $CaCl_2$ (112 mmol). To the previous solution were then added 0.4 g of D-glucose. Immediately after, the gelatin solution was stirred and kept in a hot bath ~80ºC, until gelatin was completely dissolved. The gelatin solution was then added dropwise to 200 mL of

sunflower oil, containing 1% v/v of Span® 85 and kept in a thermostatic bath at 80ºC, under stirring (600 rpm), giving rise to a w/o emulsion. Afterwards, the vessel was transferred to an iced water bath, until 15 ºC was reached. Then, 150 mL of acetone were added, so that dehydration and flocculation of the microcapsules could occur. After 10 minutes, microcapsules were filtered with a sintering glass filter. To remove any traces of oil, microcapsules were then washed with 250 mL of acetone. Afterwards, microcapsules were collected and kept in vacuum to dry, until any trace of acetone was removed. The yield was obtained according to the following equation:

$$\boldsymbol{yield = \frac{weight\ of\ the\ dried\ recovered\ material(g)}{theoretical\ weight(g)} \times 100}$$

2.2.1.2.3. Synthesis of calcium carbonate particles

Calcium carbonate particles were synthesized, at room temperature, by a precipitation method, with slight modifications to published procedures.[98][99] Na_2CO_3 and $CaCl_2$ aqueous solutions were prepared, both with a concentration of 0.5 M. The $CaCl_2$ solution was then quickly added to the Na_2CO_3 solution (in a 5:1 ratio) and kept under vigorous agitation for 5 min, with a prismatic magnetic stirrer. Afterwards, the solution was filtered and placed in the oven for 24 hours at 60ºC. The yield was obtained according to the following equation:

$$\boldsymbol{yield = \frac{weight\ of\ the\ dried\ sample(g)}{theoretical\ weight(g)} \times 100}$$

2.2.1.2.4. Substrate Coating

To obtain the final multilayer systems, capsules or particles were pre-dispersed in DCM and stirred for 15 min. Afterwards, PEI was added to achieve a percentage of 8 wt%. The solution was stirred for another 15 min and HAp pre-treated Mg1Ca alloys were then dipped for 60 s in the solution. The substrates were retrieved and left to dry at room settings for 24h to 48h. After drying, substrates were stored in a desiccator until further use. An illustration of the experimental procedure is presented in **Figure 17**.

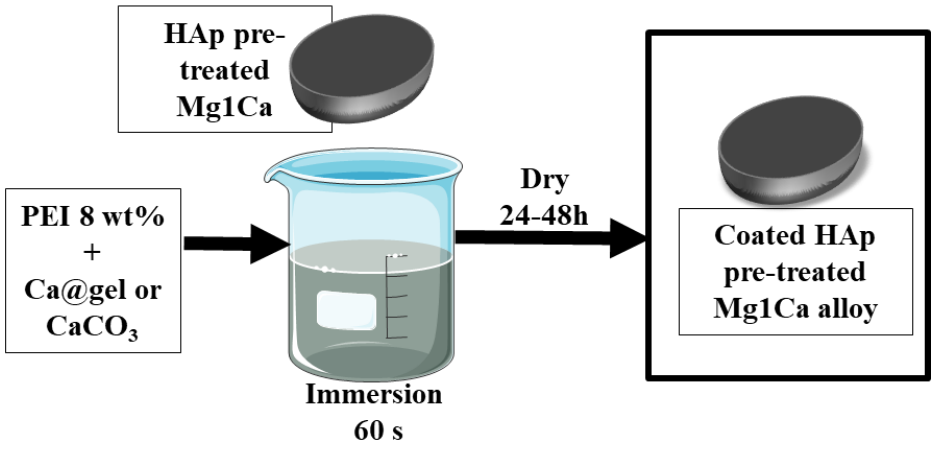

Figure 17 - Illustration of PEI coating procedure on Mg1Ca.

2.2.1.3. Surface morphology analysis (SEM- Scanning Electron Microscopy)

A small amount of the synthesized samples (gelatin capsules and calcium carbonate particles) were placed on a double-sided carbon tape. Gelatin capsules were sputtered with Gold-Palladium, for 3 min and the images were obtained while calcium carbonate particles were sputtered with a thin layer of carbon, with 2 succeeding depositions. All images were obtained with an electron beam energy of 25.0 kV, using a Hitachi S4100 scanning electron microscope.

2.2.2. Release studies

2.2.2.1 Calcium release from gelatin capsules

The encapsulation efficiency (EE) and the loading content of Ca in the gelatin microcapsules were determined. For loading content studies, a suspension of 20 mg gelatin capsules in 20 mL of distilled water was prepared and stirred, continuously, for 24 h. After this time, an aliquot was removed and centrifuged at 10000 rpm for 10 min. The supernatant was recovered and diluted, accordingly, for Atomic Absorption spectroscopy studied. The encapsulation efficiency is determined by the amount of calcium encapsulated. The loading content (LC) indicates the amount of encapsulated calcium per unit of of weight of the microparticles.

The EE was calculated by the following equation,

$$\%EE = \frac{m(Ca)_{ext}}{m(Ca)_{ini}} \times 100$$

where $m(Ca)_{ext}$ is the mass of Ca extracted from the capsules, determined by AAS, and $m(Ca)_{ini}$ is the mass of Ca initially used in the synthesis.

The LC was calculated by the following equation,

$$\%LC = \frac{m(Ca)_{ext}}{m_{Ca@gel}}$$

where $m(Ca)_{ext}$ is the mass of Ca extracted from the capsules, determined by AAS, and $m_{Ca@gel}$ is the mass of gelatin microcapsules.

Calcium release from the synthetized gelatin capsules was monitored by Atomic Absorption Spectroscopy. A suspension of 100 mg of gelatin capsules, containing calcium chloride, was prepared in triplicate, in 200 mL of deionized water. This suspension was kept under stirring (800 rpm) up to 48 hours. At different time points, an aliquot of the suspensions was retrieved and centrifuged (10000 rpm, 10 min). The volume removed was replaced with fresh deionized water. After centrifugation, the supernatant was collected and diluted for Atomic Absorption Spectroscopy, using an Avanta GBC Scientific equipment.

Due to fast swelling and release of the gelatin capsules content in aqueous environments, a 100 % release of calcium, from the capsules, was assumed at the 24 h time point. The amount of calcium released (m_t/m_∞), over time t, was determined by the following equation,[100]

$$\frac{\boldsymbol{m_t}}{\boldsymbol{m_\infty}} = \frac{\boldsymbol{V \times C_x + \sum_{i=0}^{x-1} C_i \times V_i}}{\boldsymbol{m_\infty}}$$

Where m_t represents the mass of calcium, in the medium, released at time t, m_∞ the mass of calcium in the capsules, V (L) is the volume used in the release study and V_i the volume of aliquots at a time ≠ 0. C_x and C_i correspond, respectively, to calcium mass concentrations (mg/L) at time=0 and to time ≠ 0 and x represents the total amount of aliquots withdrawn up to time t.

2.2.2.2 Calcium release from calcium carbonate particles

For loading content studies, a suspension of 20 mg $CaCO_3$ particles in 20 mL of distilled water was prepared and stirred, continuously, for 24 h. After this time, an aliquot was removed and centrifuged at 10000 rpm for 10 min. The supernatant was recovered and diluted, accordingly, for Atomic Absorption spectroscopy studies. The volume removed was replaced with fresh deionized water. The LC was calculated by the following equation,

$$\%LC = \frac{m(Ca)_{ext}}{m_{Ca@gel}}$$

where $m(Ca)_{ext}$ is the mass of Ca extracted from the capsules, determined by AAS, and $m_{Ca@gel}$ is the mass of gelatin microcapsules.

Calcium release, from the synthesized calcium carbonate particles, was monitored by Atomic Absorption Spectroscopy. A suspension of 100 mg of $CaCO_3$ particles was prepared, in triplicate, in 200 mL of deionized water. This suspension was kept under stirring (800 rpm) up to 48 hours. At different time points, an aliquot of 5 mL was removed, filtered and diluted for Atomic Absorption Spectroscopy.

The amount of calcium released (m_t/m_∞), over time t, was determined by the following equation [100]

$$\frac{\boldsymbol{m_t}}{\boldsymbol{m_\infty}} = \frac{\boldsymbol{V \times C_x + \sum_{i=0}^{x-1} C_i \times V_i}}{\boldsymbol{m_\infty}}$$

Where m_t represents the mass of calcium, in the medium, released at time t, m_∞ the mass of calcium in the capsules, V (L) is the volume used in the release study and V_i the volume of aliquots at a time ≠ 0. C_x and C_i correspond, respectively, to calcium mass concentrations (mg/L) at time=0 and to time ≠ 0 and x represents the total amount of aliquots withdrawn up to time t.

2.2.3. Assessment of biocompatibility

The biocompatibility of the prepared systems was assessed through cytotoxicity and hemocompatibility assays following the recommendations of ISO10993-5 and 10993-4, respectively. A brief scheme of the biocompatibility assay performed is presented in **Figure 18**.

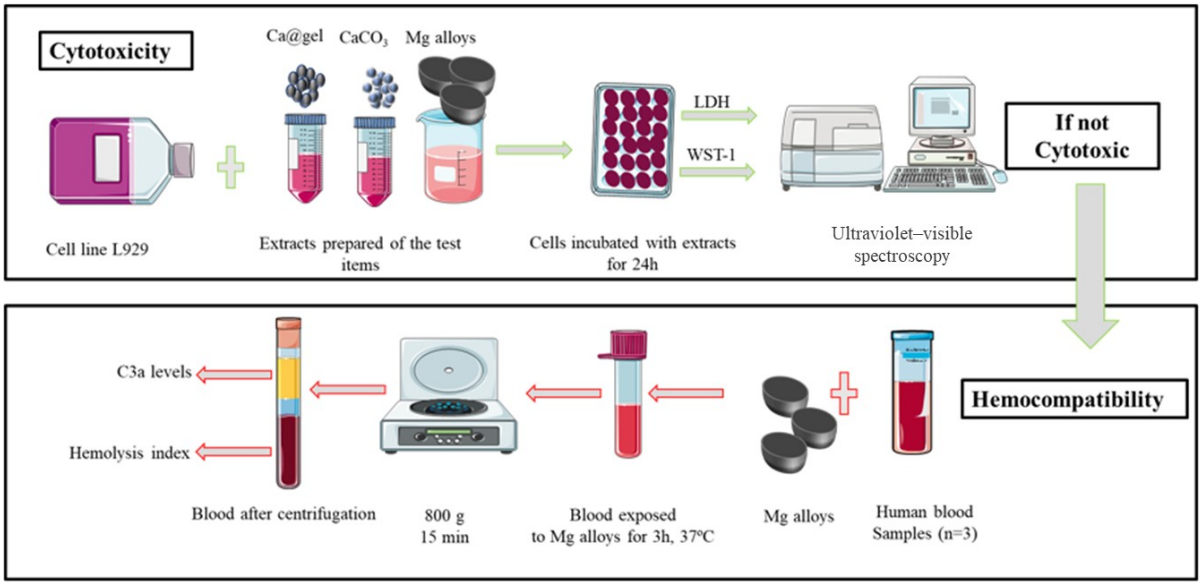

Figure 18 - Illustration of the schematic procedure used to evaluate biocompatibility, by performing cytotoxic and hemocompatibility assays.

2.2.3.1. *In vitro* cytotoxicity assessment

In this study, the cytotoxicity effects of the complete system: HAp pre-treated Mg alloys, coated with PEI with calcium carbonate particles ($CaCO_3$) or calcium loaded gelatin capsules (Ca@gel) were assessed. The cytotoxicity effects of calcium carbonate particles (0.634 mg Ca/mg) and calcium-loaded gelatin capsules (0.0238 mg Ca/mg) were also assessed.

Cytotoxicity testing of the Mg alloy extracts, and its components was evaluated *in vitro*, through indirect contact, using the fibroblast cell line L929, as recommended by ISO 10993-5:2009.[71]Two endpoints were assessed, LDH release and WST-1 reduction, at 24 h after incubation with 72-h Mg alloys extracts. Different concentrations of $CaCO_3$ particles and Ca@gel capsules were also tested for cytotoxicity at 24 h after incubation either with freshly prepared or solutions incubated for 72 h at 37ºC (same extraction conditions as the Mg alloys).

2.2.3.1.1 Extracts preparation according to ISO 10993

Mg alloys were sterilized by UV radiation, 1 h per side and kept under aseptic conditions. Preparation of extracts was carried out according to ISO 10993-12.[72] The extraction was carried out in borosilicate glass containers for 72 h at 37°C with gentle agitation (60 rpm), using MEM containing 4 mM L-glutamine, 100 units/mL of penicillin and 100 µg/mL of streptomycin as an extraction medium, at a surface area-to-extractant volume ratio of 1.25 cm^2/mL. $CaCO_3$ particles and Ca@gel were also incubated under the same conditions as the Mg alloys.

2.2.3.1.2. Cell culture and test materials exposure

L929 cells were maintained in a humidified atmosphere of 5% CO_2-95% air at 37 °C and cultured in MEM supplemented with 4 mM L-glutamine, 100 units/mL of penicillin, 100 µg/mL of streptomycin and 10% of heat-inactivated fetal bovine serum (FBS). Cells were passaged at 80% confluence using a trypsin-EDTA 0.25% solution, seeded in flat-bottom 96 well plates at a density of 10.000 cells/well and medium changed 24 h after seeding. Cells were then exposed for 24 h to the test materials at 48 h after seeding.

2.2.3.1.3. WST-1 and LDH release studies

Cytotoxicity of the test items was evaluated using the WST-1 reduction and LDH release assays. Cells incubated for 30 min with 0.2% Triton X-100 and 70% ethanol served as positive controls (PC) for the LDH release and WST-1 reduction assays, respectively. For LDH release determination, the incubation medium of each well was gently transferred to a round bottom microplate at the end of the exposure period and centrifuged for 5 min at 2000 x g to remove the cell debris. 100 µL of supernatant was gently transferred to a clean flat bottom microplate and mixed with 100 µL of the reaction mixture (freshly prepared). Absorbance was measured at 490 nm and 630 nm (reference wavelength) in a microplate reader (SpectraMax iD3, Molecular Devices, USA). Data were expressed in percentage of LDH release relative to the PC. For WST-1 reduction determination, the incubation medium was aspirated, and cells incubated for 2 h at 37 °C and 5% CO_2 with 100 µL/well of Cell Proliferation Reagent WST-1 (diluted 1:10 in FBS-free cell culture medium). Absorbance was measured at 450 nm and 630 nm (reference wavelength) in a microplate reader. Data were expressed in percentage of the negative control response.

2.2.3.2. Hemocompatibility Assessment

Hemocompatibility (hemolysis and complement activation) of the Mg alloys (Mg1Ca_HAp_PEI_Ca@gel and Mg1Ca_HAp_PEI_$CaCO_3$) was evaluated in accordance with ISO10993-4 and ASTM F756-17.[101]

2.2.3.2.1. Hemolysis index

Hemolysis induced by direct contact with the test materials was assessed by spectroscopic analysis of the hemoglobin content in plasma of a pool of healthy human volunteer donors (n=3).

Briefly, 6 mL of the pooled whole blood was diluted 1:10 in Mg-free, Ca-free PBS. Test samples were then incubated in the diluted blood at 37 ºC for 3 h in a water bath. During this incubation period, at every 30 min, the tubes were gently inverted in order to promote

contact among blood and samples. After incubation, the diluted blood was retrieved and centrifuged (800 g for 15 min). The cyanmethemoglobin method was used to determine total and free Hb concentration. Absorbance was measured at 540 nm in a microplate reader. The hemolysis index was determined conforming the following equation,

$$\%\boldsymbol{hemolysis} = \frac{|\boldsymbol{free\ Hb}|\boldsymbol{supernatant}}{|\boldsymbol{total\ Hb}|}$$

Blood incubated with 1% Triton X 100 and Mg10Gd served as positive controls. Diluted whole blood not exposed to the test samples was used as a negative control. According to ASTM F756-17, the hemolytic index obtained from test materials should be compared to the negative control results. The hemolytic grade can be determined according to **Table 6**.

Table 6- Hemolytic classification of test materials, according to the hemolytic index above the negative control. Adapted from [101].

Hemolytic Index above the negative control	**0–2**	**2–5**	**>5**
Hemolytic Grade	nonhemolytic	slightly hemolytic	hemolytic

2.2.3.2.2. Complement system activation

Complement activation was determined in plasma exposure to the test items by measuring the levels of human complement C3a fragment by ELISA.

2.2.4. Statistical analysis

Statistical analysis were performed using the GraphPad Prism 8.4.3 software. Data were tested for normality by the Shapiro-Wilk test. In all cases, if a Gaussian distribution was identified, an ANOVA statistical test was performed, followed in some cases by different multiple comparisons tests. Tukey's multiple comparison test was used to analyze the data from both release studies and from cytotoxicity assays, LDH and WST-1 data, from all test items. Dunnett's multiple comparison test was used to analyze data from the hemolysis index and C3a activation results. A p-value < 0.05 was considered significant.

Chapter3. Results and discussion

The multilayer system tested in this work was composed by a Mg1Ca alloy, an inorganic HAp layer and a polymeric PEI coating formulation with either calcium-loaded gelatin capsules or calcium carbonate particles incorporated. The multilayer system layer's is illustrated in **Figure 19**.

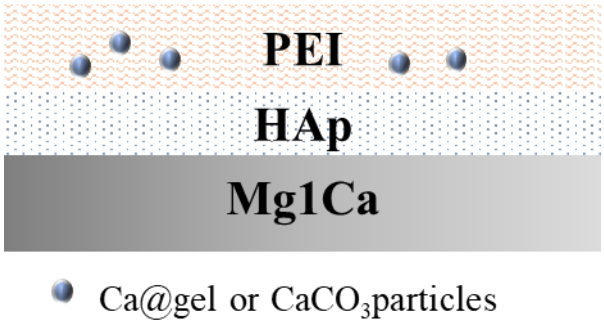

Figure 19 - Multilayer system layers representation

The selected system was developed under the MAGICOAT project (PTDC/CTM-BIO/2170/2014), in which different Mg alloys, pre-treatments and coatings were tested. The aforementioned components were chosen to integrate the final system as they demonstrated good resistance to corrosion and biocompatibility in terms of cytotoxicity.

The aim of this work was to assess the biocompatibility (cytotoxicity and hemocompatibility) of the selected final multilayer system designed in the frame of MAGICOAT project. Prior to this, it was also necessary to characterize the morphology and release profile of the Ca@gel and $CaCO_3$ particles, as well as their cytotoxicity, which is presented in the following sections.

3.1. Calcium-loaded gelatin capsules characterization

The synthesis of gelatin microcapsules was obtained with yields higher than 75%. The SEM images of the microcapsules are presented in **Figure 20**.

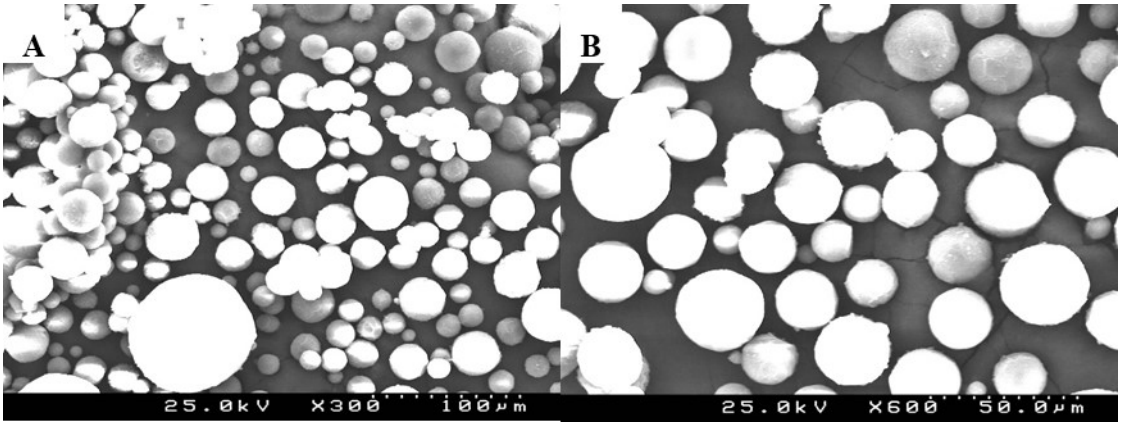

Figure 20 - SEM images of calcium-loaded gelatin capsules with a magnification of (A) x300 and (B) x600.

It is possible to observe, in **Figure 20**, that microcapsules were successfully synthesized. They present a spherical shape and heterogeneous size distribution, with an average size of ~ 25µm. Particles showed a wide range of size distribution, as seen in **Figure 20**.

Since the synthesized capsules are intended for incorporation into coatings, the broad size distribution and large size of the microcapsules may be detrimental for the properties of the final coating, considering that large capsules my disrupt its mechanical integrity.

3.1.1. Release studies

Before carrying out the release studies, the encapsulation efficiency (EE) and the loading content of Ca in the gelatin microcapsules were determined. An encapsulation efficiency close to 90% and a loading content of 2.38% were obtained.

In what concerns the release studies, an ANOVA statistical analysis was performed, to the replicates data, after a normality test, that showed a Gaussian distribution and allowed the determination of a statistical significance, since a p-value of 0.042 was obtained. With a multiple comparison test (Tukey's), it was possible to identify which of the replicates was statistically significantly different and the obtained results are presented in **Table 7**.

Table 7 - Adjusted p-values and the respective significance of different comparison tests.

Tukey's multiple comparisons test	Adjusted p-value	Significant
Ca@gel#1 vs. Ca@gel#2	0.0086	Yes
Ca@gel#1 vs. Ca@gel#3	0.9975	No
Ca@gel#2 vs. Ca@gel#3	0.0488	Yes

According to the results, only replicates 1 and 3 presented a non-significant statistical difference, with $p > 0.05$. The other replicate comparisons presented $p < 0.05$ and were, therefore, considered statistically significant from each other thus, only replicates 1 and 3 were used to plot the percentage of the cumulative release of calcium. The release profile of calcium-loaded gelatin microcapsules is presented in **Figure 21**.

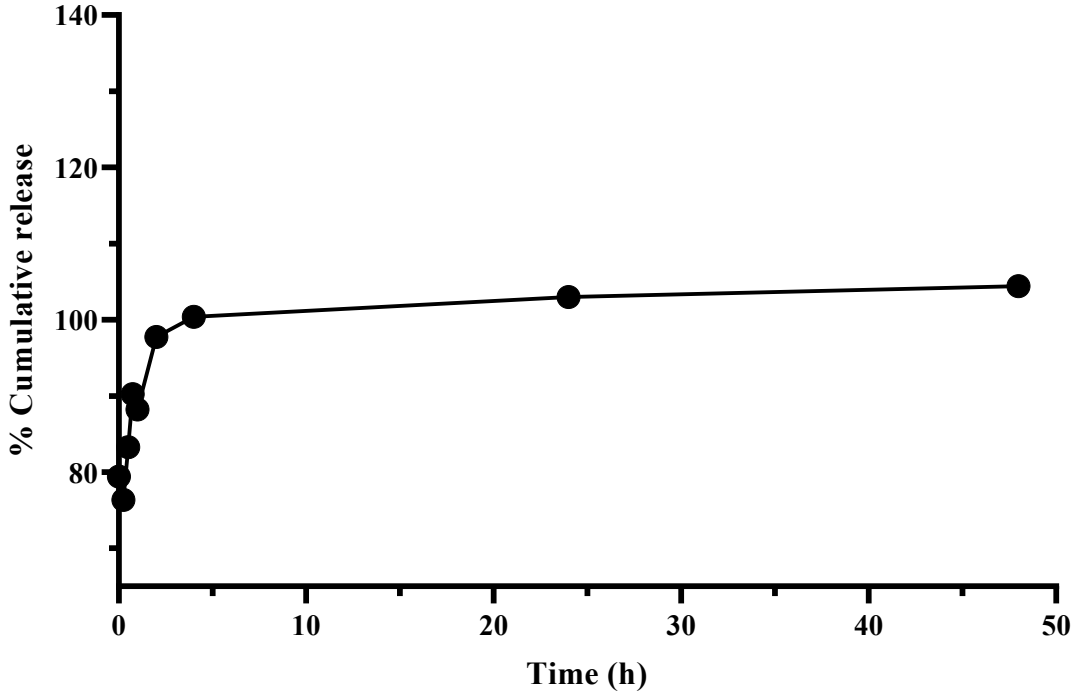

Figure 21 - Calcium release profile from gelatin microcapsules for a period of 48 h.

The release profile depicted in **Figure 21**, shows a high burst release of calcium immediately after immersion in the aqueous medium, with microcapsules releasing ~80% of its contents. The total amount of calcium was released up to 4 hours. Gelatin is known for its propensity to swell in aqueous environments due to hydration. This swelling might result in an increase of chain mobility which, in turn, might increase and promote a high rate release of calcium by diffusion, through the polymer, if the crosslinking is not efficient. The observed burst release of calcium from microcapsules is most likely due, not only for its propensity to swell, but also to the low concentration of the crosslinking agent, which was not enough to avoid capsules' swelling. D-Glucose was the crosslinker used and is responsible for promoting cross-linking interactions in the Ca@gel prepared. By increasing the amount of D-glucose, or extending the crosslinking reaction time, denser bridges might be formed between the polymer chains, increasing the crosslinking degree leading to more stable and rigid spheres. Therefore,

solvent permeability would have been reduced which would have led to a more controlled release of the capsules' contents.[102]

Even though a burst release of calcium from the capsules occurs, they still show potential as delivery systems. By optimizing the synthesis, they may be promising as drug delivery system for applications that require a more controlled release of the active species encapsulated. Apart from calcium, that is known to promote bone healing and growth, other active species may be encapsulated according to the intended application of the outer layer of the studied system (substrate protection, decrease of the secondary effects in *in vivo* conditions).

3.2. Calcium carbonate particles characterization

Calcium carbonate particles were obtained by a precipitation method, with yields between 80-90%. Particles were analyzed by SEM and the images obtained are presented in **Figure 22**.

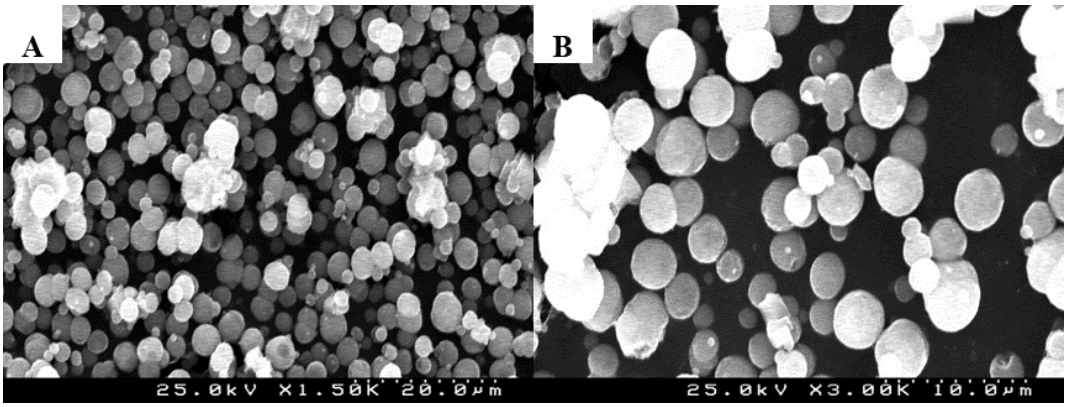

Figure 22 - SEM images of calcium carbonate particles with a magnification of (A) x 1.50k and (B) x3.00k.

It is possible to observe that particles present a spherical shape and a relatively homogeneous size, with sizes comprised between 0.7 - 5.0 µm. As it is known, calcium carbonate can precipitate in different phases: one amorphous phase and three crystalline phases (vaterite, calcite and aragonite).[66] Cubic shapes are known to be calcite, the most thermodynamically stable phase of $CaCO_3$ [106][107], whereas particles with a spherical shape are known as vaterite, polymorph with lower thermodynamic stability than calcite. The presence of spherical shaped particles, in **Figure 22**, indicates that vaterite was the polymorph synthetized.

Vaterite is the most promising polymorph to be used as a drug delivery carrier, due to its higher solubility in water, biological inertness, low cytotoxicity and ability to form polycrystalline aggregates with higher porosity and surface area. This can lead to a higher

loading capacity and potential release of the active species.[66] Spherical vaterite has shown potential in the biomedical field, being applied in regenerative medicine and tissue engineering, among other applications.[103]

3.2.1. Release studies

In order to determine the calcium release over time, the total amount of calcium in the particles was determined by atomic absorption spectroscopy (AAS). The results showed a loading content of 63.4%. The release profile of Ca^{2+} from $CaCO_3$ particles was monitored by AAS for a period of 48 hours and is presented in **Figure 23**.

By performing an ANOVA test, a p-value of 0.0204 was obtained which means that there were significant differences between the replicates at the same time points. By performing a multiple comparison test (Turkey's), it was not possible to determine, with certainty, which sample presented significant differences, possible of being excluded and therefore no replicate was excluded, and all 3 replicas were used in calculations.

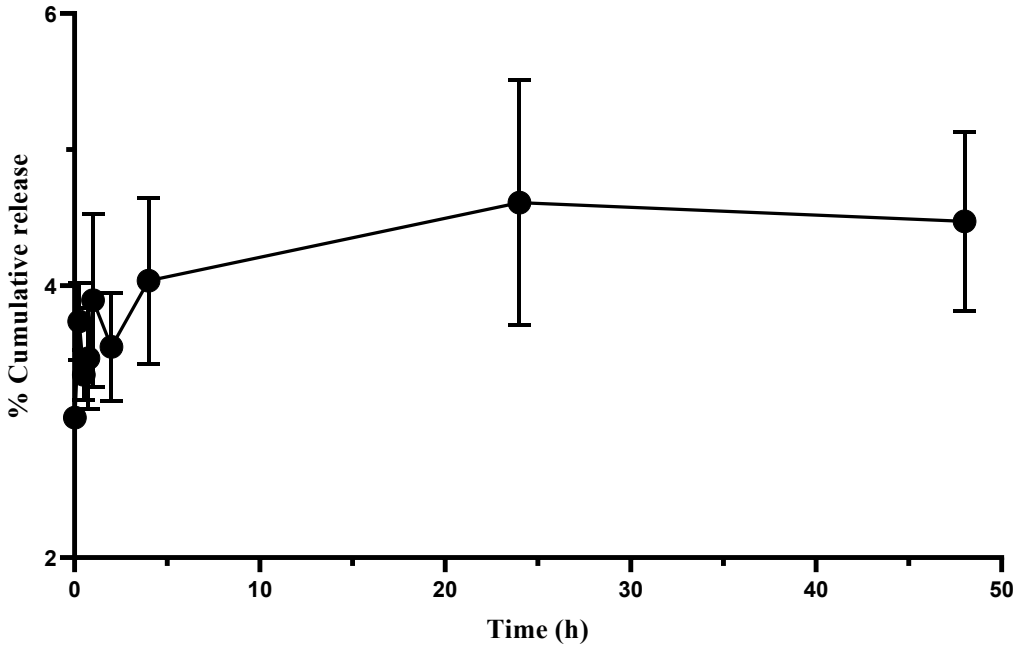

Figure 23 - Calcium release profile from $CaCO_3$ particles for a period of 48 hours. Results show 3 independent measures at each time point.

The calcium release data in **Figure 23** shows high standard deviations, probably due to the very low absorbance observed.

The release of calcium from the $CaCO_3$ particles is mainly controlled by the dissolution of the particles in water. The release profile shows very low release, with only approximately

5% of calcium released up to 48 h of immersion. It is also possible to observe that there is no significant increase in calcium release, up to 4 hours, conforming the limitation in release by the solubility of the particles.

3.3 Biocompatibility analysis

3.3.1 Cytotoxicity analysis

The cytotoxicity of extracts of the complete systems (Mg1Ca_HAp_PEI_Ca@gel and Mg1Ca_HAp_PEI_$CaCO_3$) was evaluated. Freshly prepared and 72-hour extracts of the gelatin microcapsules containing calcium (Ca@gel) and calcium carbonate particles ($CaCO_3$) were also tested for cytotoxicity. The aspect of the 72-hour extracts of the tested Mg1Ca alloys, Ca@gel and $CaCO_3$ particles is shown in **Figure 24.** As depicted, no evident signs of corrosion were observed in both Mg1Ca_HAp_PEI_Ca@gel and Mg1Ca_HAp_PEI _$CaCO_3$, except for some gas bubbles which may be associated with hydrogen evolution.

Figure 24 - General aspect of the tested 72-hour extracts. From left to right: $CaCO_3$ particles, Ca@gel capsules, Mg1Ca_HAp_PEI_Ca@gel and Mg1Ca_HAp_PEI _$CaCO_3$.

3.3.1.1. Gelatin microcapsules (Ca@gel) and calcium carbonate ($CaCO_3$) particles

The evaluation of Ca@gel and $CaCO_3$ particles cytotoxicity is important to guarantee that they are not toxic, and therefore can be added as reservoirs for active species to the designed system. The effect on membrane integrity and cell metabolic activity, caused by incubation for 24 h with Ca@gel in L929 cells is shown in **Figure 25.**

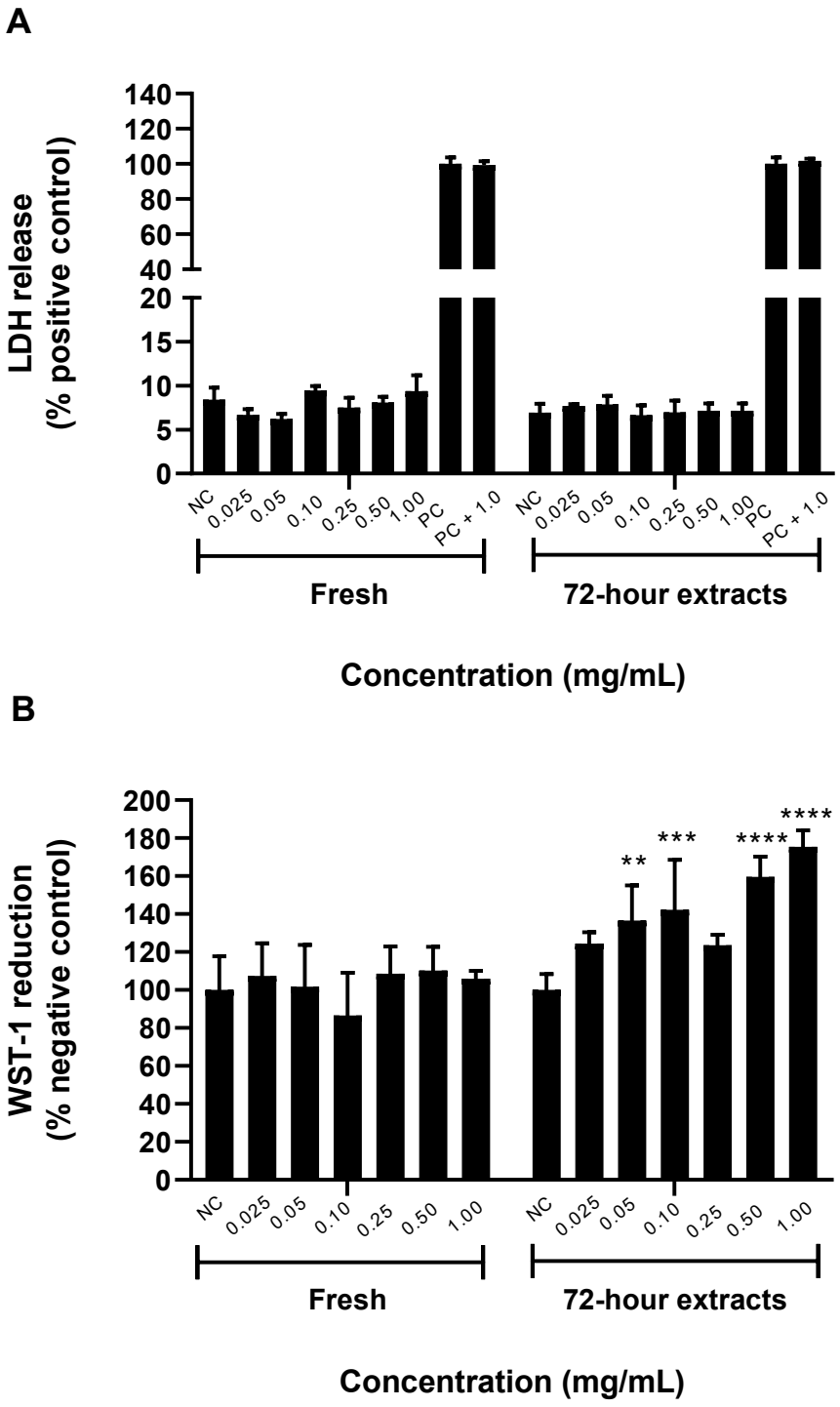

Figure 25 - In vitro cytotoxicity of Ca@gel in L929 cells as assessed by the LDH release (A) and WST-1 reduction (B) assays. Cells were exposed for 24 h to varied concentrations (0,025 – 1 mg/mL) of freshly prepared or 72-hour extracts of Ca@gel. Data is expressed as mean ± SD. **p < 0.01; ***p < 0.001, ****p < 0.0001 *vs* the respective NC.

Figure 25A presents the % of LDH release relative to the positive control, i.e. cells lysed with 0.2 % Triton X100, in L929 cells at 24 h after incubation with freshly prepared or

72-hour extracts of Ca@gel. As shown in **Figure 25A**, all the tested concentrations of Ca@gel, either the freshly prepared suspensions or the 72-hour extracts, did not induce any significant cytototoxicity as compared to the negative control (NC), i.e. did not affect the integrity of the plasma membrane of L929 cells at 24 h after exposure.

The metabolic capacity of L929 cells at 24 h after exposure to the Ca@gel was also evaluated by the WST-1 reduction assay. As displayed in **Figure 25B**, Ca@gel did not decrease cell metabolic activity at any tested concentration. In fact, a significant increase in WST-1 reduction was detected for all Ca@gel concentrations (except 0,025 and 0,25 mg/mL), for the 72-hour extracts. This finding can be explained by the contribution of the main components of the Ca@gel gelatin: calcium and glucose. Glucose, a sugar, can provide energy so that cells can carry out their metabolic activities. By allowing cells to have an additional source of glucose, provided by the microcapsules, the cells have an extra source of carbon to use in their metabolic activity.[105] Calcium in the microcapsules, as already mentioned, is involved in a large number of cell functions, and has also been studied for having an influence in cell proliferation, by helping cells to attach to substrate.[106] Gelatin is originated from collagen (a protein found in bone, skin and connective tissue), has a natural source and it is known to be very biocompatible. Thus, WST-1 assay results are in accordance with the LDH results, supporting the view that Ca@gel are not cytotoxic to L929 cells at the tested concentration range.

LDH release and WST-1 reduction in L929 cells exposed to the $CaCO_3$ particles were also assessed and data are presented in **Figure 26**.

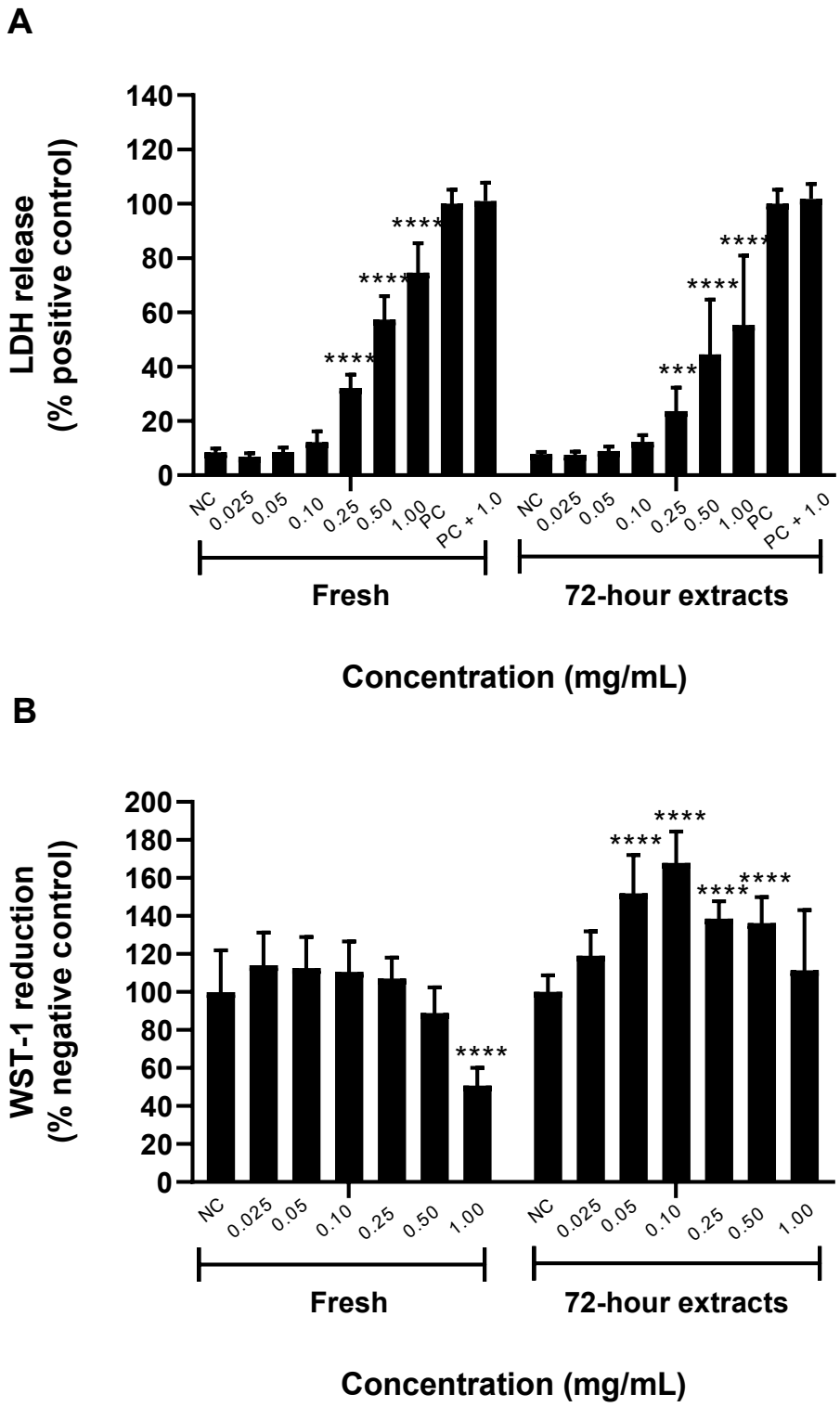

Figure 26 - In vitro cytotoxicity of $CaCO_3$ particles in L929 cells as assessed by the LDH release (A) and WST-1 reduction (B) assays. Cells were exposed for 24 h to varied concentrations (0,025 – 1 mg/mL) of freshly prepared or 72-hour extracts of $CaCO_3$ particles. Data is expressed as mean ± SD. ***p < 0.001, ****p < 0.0001 *vs* the respective NC.

A concentration-dependent increase in LDH extracellular content was observed in cells incubated for 24 h with $CaCO_3$ particles fresh suspensions and extracts up to values close to 80% relative to the positive control (maximum release) **(Figure 26A)**. In addition, the levels of LDH released in control cells were rather low, varying between 5 to 7% of the positive control, which is indicative of a healthy cell monolayer.

Regarding the WST-1 reduction assay, only the highest tested concentration of the fresh suspension of $CaCO_3$ particles was able to significantly reduce cell metabolic activity (**Figure 26B)**, which contrasts with the concentration-dependent increase observed for the LDH release under the same experimental conditions **(Figure 26A)**. Cells exposed to the 72-hour extracts of $CaCO_3$ particles also exhibited increased WST-1 reduction, again contrasting with the LDH release data. Considering that LDH assay is a biomarker of late toxicity, as it indicates loss of plasma membrane integrity, the contradicting cell metabolic activity results might be explained by some interference of the $CaCO_3$ particles in the WST-1 assay. Nevertheless, the tested concentrations of both Ca@gel and $CaCO_3$ particles are far beyond the levels expected to be present in the Mg alloys coating.

3.3.1.2. Multilayer system (inclusion of particles or capsules in the coating)

The cytotoxicity of the complete multilayer system, with either Ca@gel or $CaCO_3$ particles, was evaluated. The extracts were prepared by incubating the complete systems with an extraction medium for 72 h at 37 ºC and tested for cytotoxicity in different extract dilutions using the L929 cell line. The results of the LDH assay performed are presented in **Figure 27**.

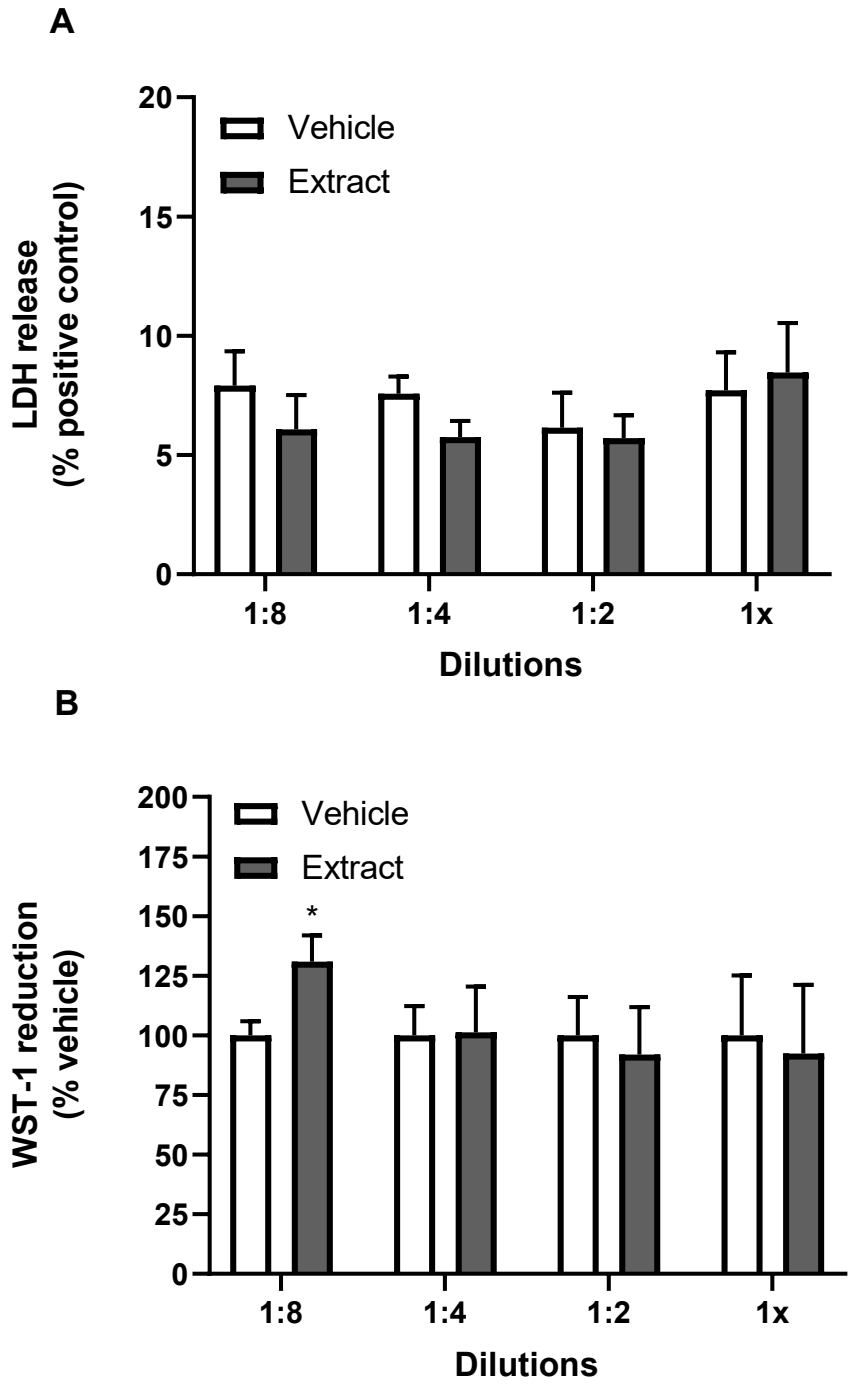

Figure 27 - In vitro cytotoxicity of Mg1Ca_ HAp_ PEI_Ca@gel in L929 cells as assessed by the LDH release (A) and WST-1 reduction (B) assays. Cells were exposed for 24 h to different dilutions of the 72-hour extract of Mg1Ca _HAp_ PEI_Ca@gel. The vehicle represents the extraction medium used, incubated for 72 hours without the test item. Data is expressed as mean ± SD. Data was analyzed by the one-way analysis of variance (ANOVA) test followed by the Tukey's post hoc test for multiple comparisons. *$p < 0.05$ vs the respective vehicle.

As shown in **Figure 27A**, the percentage of LDH released from cells, when in contact with the 72-hour extracts obtained from the Mg1Ca_HAp_ PEI _Ca@gel system is less than 10% in all tested dilutions of the extracts. No significant changes in LDH release were detected in cells exposed for 24 h to different dilutions of the 72-hour Mg1Ca_HAp_ PEI _Ca@gel extract as compared to the respective vehicle (extract medium diluted in the same percentage). On the other hand, no changes in the cellular metabolic activity were found with the exception of the 1:8 extract dilution that significantly increased the WST-1 reduction levels to values around 125% of the respective vehicle (**Figure 27B**).

Regarding the Mg1Ca_HAp_ PEI _$CaCO_3$ system extracts, as depicted in **Figure 28A,** no significant changes in the levels of LDH released as compared to the respective vehicles were detected, with values below 10% of PC (total LDH release). At the same time, no significant changes in the cell metabolic activity were observed under the same experimental conditions (**Figure 28B**).

Taken together, these data indicate that Mg1Ca_HAp_PEI_Ca@gel and Mg1Ca_HAp_PEI_$CaCO_3$ are non-cytotoxic. Also, previous cytotoxicity testing of bare or Mg1Ca_HAp extracts (results not shown) carried out under the MAGICOAT project, confirm the view that these alloys are biocompatible.[107]

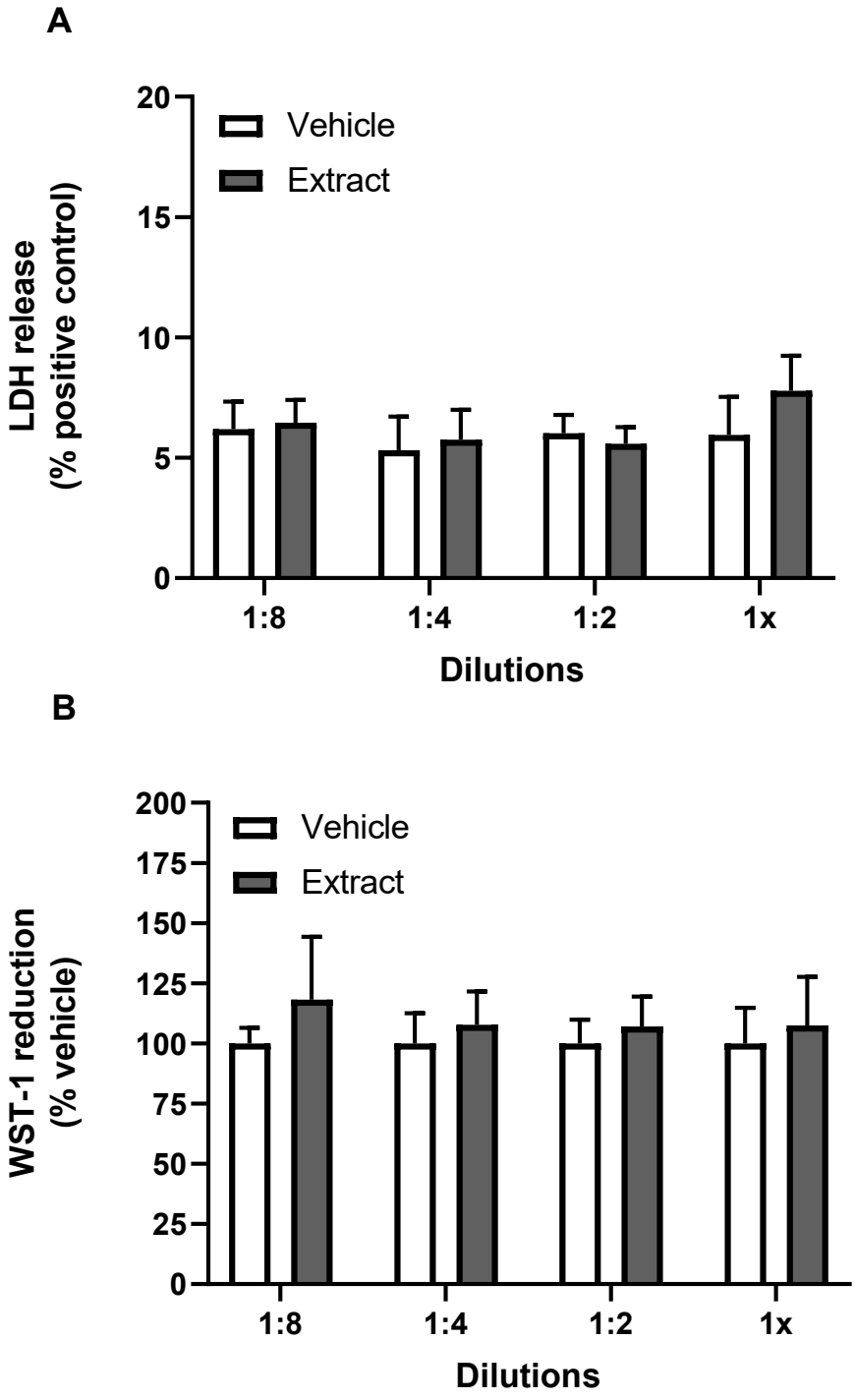

Figure 28 - In vitro cytotoxicity of Mg1Ca_ HAp_PEI_$CaCO_3$ in L929 cells as assessed by the LDH release (A) and WST-1 reduction (B) assays. Cells were exposed for 24 h to different dilutions of the 72-hour extract of Mg1Ca_ HAp_PEI_$CaCO_3$. The vehicle represents the extraction media used, incubated for 72 hours without the test item. Data is expressed as mean ± S D. Data was analyzed by the one-way analysis of variance (ANOVA) test followed by the Tukey's post hoc test for multiple comparisons. No significant differences were found.

The majority of Mg alloys designed for biomedical implants in the orthopedical field have been found to exhibit good biocompatibility. However, Mg1Ca alloy for biomedical application are still scarce and therefore, very few information is available on their biocompatibility nature. One of these few studies, was performed by Xiong et al [108], that investigated the effects of a coated Mg1Ca on MC3T3-E1 cells viability. The coating was composed by a fluor-based conversion film, silk-phytic acid coating, and silk fibroin coating. Silk-phytic acid coating was loaded as a corrosion inhibitor by dissolving Mg^{2+} and Ca^{2+} ions. The mitochondrial activity assay and live/dead tests were performed, and both showed good results. The live/dead showed higher number of live cells when comparing to cells exposed to the bare Mg1Ca alloy. The overall system was considered noncytotoxic and promoted cell proliferation.[108] Similar behavior was found in the multilayer systems in this work, with cells showing no signs of damage to cell membrane, and high levels of WST-1 reduction and therefore cell metabolic activity.

One of the most utilized alloys in orthopedical applications is the AZ31 alloy, thus more information on its cytotoxicity behavior is available. Among the most recent studies, Abdal-Hay et al. studied the effects of an AZ31 Mg alloy, sprayed with membrane films of pristine and hydroxyapatite-doped poly (lactic acid) on MC3T3 cells viability. No significant changes in cell viability, as assessed by the MTT assay, were detected with the number of cells increasing over time.[109]

Sikder et al also studied AZ31 coated with a fluorine-doped hydroxyapatite (FHA) coating or a bilayer coating of FHA and poly (lactic acid) (FHA–PLA). Cell viability was assessed by the MTT assay at 1, 4 and 7 days after exposure to the AZ31extract in MC3T3-E1 pre-osteoblasts. Results showed that AZ31-FHA significantly increased cell viability when compared to cells exposed to the AZ31 bare alloy.[110] Lin et al also evaluated the effects of a polydopamine-coated AZ31 alloy in the cell viability and morphology of mouse L929 fibroblasts.[111] The cytotoxicity tests demonstrated that the AZ31 system did not cause a cytotoxic response in L-929 cells and cell growth was also promoted.

Parande et al studied the biosafety of Mg-2.5Zn alloys coated with silicon and hydroxyapatite. The cytotoxicity of the alloys was tested in MC3T3E1 cells by the LDH assay, after an incubation period of 24 h. Results showed that the addition of silicon and hydroxyapatite decreased the cytotoxicity of the bare alloy used.[112]

Kim et al investigated the cytotoxic effects of dense or porous PEI-coated Mg pure alloys and compared those results to AZ31 alloys. Cell proliferation, differentiation and attachment were evaluated in response to the pure Mg and PEI-coated Mg alloys on a

preosteoblast cell line (MC3T3-E1). All results proved that PEI highly increased the biocompatibility of the Mg alloys.[113] This study demonstrated the potential of PEI to improve biocompatibility by controlling the corrosion rate, which is in accordance with the results present in this work, where the PEI coating did not cause any cytotoxicity, and improved the system cytocompatibility, when compared to the bare Mg1Ca alloy and Mg1Ca_HAp system.[107]

The majority of the studies where HAp was applied showed very good biocompatibility. PEI coatings on Mg alloys are very less reported in literature, nevertheless, the existing ones show great potential and no major cytotoxic effects. However, cytocompatibility alone does not guarantee that no adverse reaction will occur. The material may be in contact with blood and therefore requires a hemocompatibility test, to assure that no adverse reactions will occur when the material is in contact with blood.

3.3.2 Hemotoxicity results

3.3.2.1. Hemolysis index

The hemolysis index of the multilayer systems was calculated based on the free Hb content following incubation for 3 h at 37 °C. In **Figure 29** is shown the aspect of the centrifuged blood samples after direct contact with the test items.

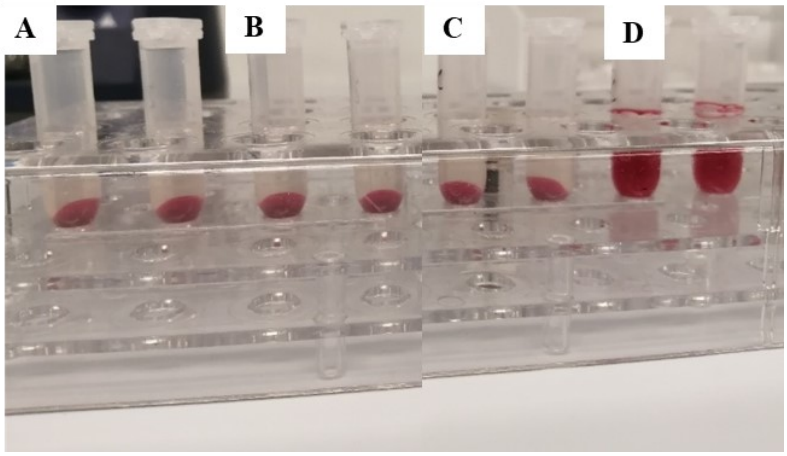

Figure 29 - Aspect of the centrifuged blood samples after direct contact with test samples: (A) Mg1Ca_HAp_PEI_Ca@gel, (B) Mg1Ca_HAp_PEI_$CaCO_3$, (C) Negative controls and (D) Positive controls.

The ASTM F756-17 standard [101], classifies the material as non-hemolytic (0–2% of hemolysis), slightly hemolytic (2–5% of hemolysis) and hemolytic (>5% of hemolysis). Accordingly, as shown in **Table 8**, Mg1Ca_HAp_PEI_$CaCO_3$ and Mg1Ca_HAp_PEI_Ca@gel are classified as non-hemolytic. The Mg10Gd, which has been

used as a positive control alloy based on the cytotoxicity findings, presented an high hemolysis index, reaching 34.52%, being classified as an hemolytic alloy.

Table 8 - Blood hemolysis index after direct contact with the tested Mg1Ca-based systems.

	Free Hb (mg/mL)	Total Hb (mg/mL)	% Hemolysis index
Negative Control (NC)	0.03 ± 0.01	7.90 ± 0.18	0.33 ± 0.13
Mg1Ca_HAp_PEI_Ca@gel	0.03 ± 0.01	6.93 ± 0.44	0.38 ± 0.06
Mg1Ca_HAp_PEI_$CaCO_3$	0.03 ± 0.001	6.42 ± 0.72	0.48 ± 0.08
Mg10Gd	2.66	7.71	34.52
Positive Control (PC)	8.24	7.86	104.82

Data is expressed as mean ± SD (n=1-2). NC - negative control; PC - positive control (1% Triton X-100).

3.3.2.2. Complement system activation

The complement system plays an important role in the body's immune response. Measurement of complement protein C3a levels is a widely used complement activation marker. Thus, C3a levels were quantified by ELISA in plasma samples isolated from citrate anticoagulated blood exposed to the tested Mg alloys. As depicted in **Figure 30**, no significant changes in C3a levels of blood samples incubated with either Mg1Ca_HAp_$CaCO_3$ or Mg1Ca_HAp_PEI_Ca@gel were detected as compared to the NC.

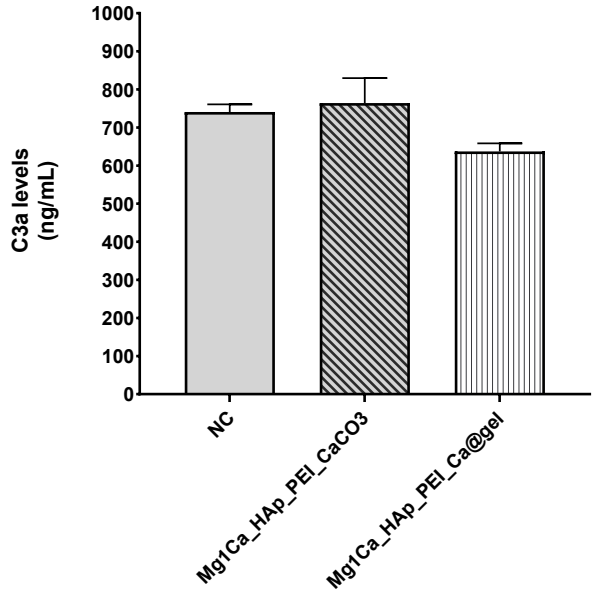

Figure 30 - Complement C3a protein levels in human plasma after direct contact with the tested alloys: Mg1Ca_HAp_PEI_$CaCO_3$ and Mg1Ca_HAp_PEI_Ca@gel. Data represent the mean ± standard deviation (SD) and was analyzed using one-way ANOVA followed by Dunnett's test.

Overall, our data supports the view that both multilayer systems are hemocompatible. Nevertheless, it is important to keep in mind that *in vitro* hemocompatibility might not accurately predict *in vivo* hemocompatibility, namely the long-term effects or blood/device interactions of a complex kind. Good hemocompatibility is an essential requirement for implant materials, especially for biodegradable Mg alloys, which could change the *in situ* environment after implanted. Reports on the hemocompatibility of Mg1Ca alloys are very scarce. In this regard, Liu et al [114] investigated the biocompatibility of five different types of sterilization in MgCa alloys: steam autoclave sterilization, ethylene oxide steam sterilization , glutaraldehyde sterilization , dry heat sterilization and Co60 γ ray radiation sterilization . Steam autoclave sterilization reduced the hemolysis ratio of pure Mg and MgCa alloys, to less than 5 %, while the hemolysis percentage significantly increased with the other four sterilization processes, reaching 80 % of hemolysis ratio. The high difference between Mg1Ca_HAp and the polished MgCa alloy hemolysis ratio might suggest that the HAp pre-treatment on MgCa alloys might increase hemocompatibility. Indeed, HAp that is one of the components of the tested multilayer systems was found to be very biocompatible and has demonstrated a non-hemolytic behavior. Ooi et al. [115] carried out a study on the hemocompatibility of nanoporous HAp prepared using two non-ionic surfactants, Pluronic P123 and F127. These authors reported that nanoporous HAp induced less than 5% hemolysis, suggesting that the material is highly hemocompatible. In addition, no activation and morphological change was observed on the platelets adhered onto the HAp.[115]

In the present study, PEI was also incorporated in the final multilayer system. Cerda-Cristerna et al. evaluated the hemocompatibility of varied concentrations (10, 100, 200, 500 and 1000 μg / mL) of PEI incubated for different periods of time (15, 60, 120 and 240 min).[116] These authors showed that only exposure for 240 min to 1000 μg/mL induced hemolysis with values of the free hemoglobin was higher than 5%.[116]

Zhen and al. studied the influence of the Mg ions concentration and pH in the hemolysis.[117] They observed that concentrations up to 1000 μg/ml Mg^{2+} did not cause hemolysis, but hemolysis reached 53.8% when pH > 11. Therefore, hemolysis seems to be dictated by pH changes rather than increases of the Mg^{2+} levels. In the present study, considering the low hemolysis index of both multilayers systems is likely that very low concentrations of Mg ions have been released and no significant changes in the blood pH occurred under our experimental conditions.

So far, a variety of different systems have been developed to improve the biocompatibility and corrosion resistance of Mg alloys. However, most of the studies have

focused on the cytocompatibility, lacking evidence of their safe interaction with human blood. Nevertheless, some of the systems developed and tested for hemocompatibility showed good results, but none have a design with similar components and assembly as the system tested in this work.

AZ31 appears to be the most widely studied implant material. Wei et al. [37] and Wang et al. [118] studied the effect of the polymeric coating (plasma electrolytic oxidized/ poly(L-lactide) (PEO/PLLA) composite and Si-containing coating (Mg_2SiO_4, MgO and SiO_2 , respectively) on hemocompatibility of AZ31 alloys. In both studies, the hemocompatibility of the Mg alloys was improved by coating the alloy with the selected polymer, with hemolysis ratios lower than 2 %. The same occurred when PEI was added to our Mg1Ca_HAp alloy, which decreased its hemolysis index and activation of C3a.[107]

Guan et al investigated the degradation, hemolysis, and cytotoxicity of Mg-4.0Zn-1.0Ca-0.6Zr alloys coated with HAp.[53]Hydroxyapatite is one of the elements common to the multilayer system studied in our work. These authors showed that HAp coating initially decreased the concentration of Mg ions released inducing hemolysis ratios below 5 %. In the present study, the hemolysis indices of both systems were below this value, most likely due to the different alloying elements present in both systems.

Singh et al [119], developed a nanocomposite coating of hydroxyapatite-bioglass-chitosan with Fe_3O_4 NPs for AZ91. The coating significantly decreased the AZ91 hemolysis index for approximately 8 % to 4 %, showing that the superficial layer is important for the device cellular interactions and toxicity.

Chapter 4: Conclusions

In this work, a Mg1Ca alloy, pre-treated with HAp, coated with PEI, with Ca@gel or $CaCO_3$, developed in the frame of MAGICOAT project (PTDC/CTM-BIO/2170/2014), was prepared and its biocompatibility was assessed, in what concerns its *in vitro* cytotoxicity and hemocompatibility.

As Ca@gel and $CaCO_3$ particles were to be included in the PEI coating it was crucial to evaluate their release profile, observe their morphology and assess their cytotoxicity prior to the biocompatibility assays of the complete system. The gelatin capsules showed a spherical shape and their release profile displayed a high burst release of calcium immediately after immersion achieving a complete release after 48 h, most probably due to the low crosslinking degree in the microcapsules. When tested for its cytotoxicity, Ca@gel showed low percentages of LDH release and a high percentage of WST-1 reduction, which suggests that Ca@gel induced very low cell damage and high cell proliferation therefore being classified as non-toxic.

The synthesized $CaCO_3$ particles also presented a spherical shape, confirming the formation of vaterite. Release studies showed a very low release probably due to the limited solubility of the particles in water. As to their cytotoxicity, a concentration-dependent increase in LDH release was observed, indicating that plasma membrane has been compromised. Nevertheless, this effect was detected for concentrations much greater than the one found in the complete system, therefore not compromising their use in the final system.

After microcapsule and particle characterization, the biocompatibility of the studied systems was evaluated. Systems with either the addition of Ca@gel or $CaCO_3$ particles to the PEI coating (Mg1Ca_HAp_PEI_Ca@gel and Mg1Ca_HAp_PEI_$CaCO_3$) were tested for their cytocompatibility. The results showed that both systems are non-toxic and, when compared to the cytocompatibility results previously obtained under the project MAGICOAT for Mg1Ca_HAp and Mg1Ca_HAp_PEI, they have higher cytocompatibility, suggesting that the addition of microcapsules or particles contributed to an improvement of the cytocompatibility of the multilayered system.

Finally, the Mg1Ca_HAp_PEI_Ca@gel and Mg1Ca_HAp_PEI_$CaCO_3$ systems were evaluated for their hemocompatibility. Under our experimental conditions, no significant hemolysis has been detected and both systems are classified as non-hemolytic according with the criteria established in ASTM F756-17 standard.

Regarding an eventual activation of the immune system in response to the contact of the systems with the blood, our results seem to suggest that no significant immune response was triggered in vitro, as the levels of C3a, an important effector of the complement system, were not significant different from the NC.

Overall, the developed multilayer system, presented a good *in vitro* biocompatibility behavior, inflicting no harm in L929 cell line and proving to be a hemocompatible material. It is important to stress the outmost importance of performing *in vivo* tests, since *in vitro* tests might not truly represent interactions between blood/ device for longer periods of time. Nevertheless, with the tests performed in this work and with further optimization as well as future *in vivo* tests it is possible to infer that this system has a high potential to be used in the future as a biomaterial-based implant in the orthopedical field.

Thus, the objectives proposed in this work, the evaluation of cytotoxicity and hemocompatibility of the multilayer system, were achieved with good biocompatibility results, suggesting a great potential of this system as an implant material in the orthopedical area, in the future.

Future Perspectives

In the future, some optimizations and further investigation can be conducted to better understand and to improve the biocompatibility and corrosion rate control of the multilayer system produced.

It is known that nanoparticles present higher surface area and higher bioavailability, than capsules with larger sizes.[120] In the future, in order to use the synthesized capsules in coatings as well as drug delivery systems, a smaller particle size (in the nanometre order) would be desired, in order to ensure a higher surface area, availability and higher cellular uptake of the bioactive species. Also, other active species may be introduced in the gelatin particles, with properties that may me important and essential to each patient.

It would also be essential, to investigate the mechanical properties of the system, as well as new electrochemical and *in vitro* biocompatibility assays, with conditions more similar to the ones found in the human body.

Since the *in vitro* biocompatibility assays showed good results, in the future, *in vivo* tests might be performed to further investigate the multilayer system.

Bibliographic references

[1] M. Niinomi, "Recent research and development in metallic materials for biomedical, dental and healthcare products applications," *Mater. Sci. Forum*, vol. 539–543, no. PART 1, pp. 193–200, 2007.

[2] P. Tian and X. Liu, "Surface modification of biodegradable magnesium and its alloys for biomedical applications," *Regen. Biomater.*, vol. 2, no. 2, pp. 135–151, 2015.

[3] F. Rosalbino, S. De Negri, A. Saccone, E. Angelini, and S. Delfino, "Bio-corrosion characterization of Mg-Zn-X (X = Ca, Mn, Si) alloys for biomedical applications," *J. Mater. Sci. Mater. Med.*, vol. 21, no. 4, pp. 1091–1098, 2010.

[4] J. A. Lyndon, B. J. Boyd, and N. Birbilis, "Metallic implant drug/device combinations for controlled drug release in orthopaedic applications," *J. Control. Release*, vol. 179, no. 1, pp. 63–75, 2014.

[5] J. Yang, F. Cui, and I. S. Lee, "Surface modifications of magnesium alloys for biomedical applications," *Ann. Biomed. Eng.*, vol. 39, no. 7, pp. 1857–1871, 2011.

[6] B. Denkena and A. Lucas, "Biocompatible magnesium alloys as absorbable implant materials adjusted surface and subsurface properties by machining processes," *CIRP Ann. - Manuf. Technol.*, vol. 56, no. 1, pp. 113–116, 2007.

[7] E. Zhang, L. Yang, J. Xu, and H. Chen, "Microstructure, mechanical properties and bio-corrosion properties of Mg-Si(-Ca, Zn) alloy for biomedical application," *Acta Biomater.*, vol. 6, no. 5, pp. 1756–1762, 2010.

[8] M. I. Sabir, X. Xu, and L. Li, "A review on biodegradable polymeric materials for bone tissue engineering applications," *J. Mater. Sci.*, vol. 44, no. 21, pp. 5713–5724, 2009.

[9] N. Li and Y. Zheng, "Novel Magnesium Alloys Developed for Biomedical Application: A Review," *J. Mater. Sci. Technol.*, vol. 29, no. 6, pp. 489–502, 2013.

[10] S. Shadanbaz and G. J. Dias, "Calcium phosphate coatings on magnesium alloys for biomedical applications: A review," *Acta Biomater.*, vol. 8, no. 1, pp. 20–30, 2012.

[11] L. Tan, J. Dong, J. Chen, and K. Yang, "Development of magnesium alloys for biomedical applications: structure, process to property relationship," *Mater. Technol.*, vol. 33, no. 3, pp. 235–243, 2018.

[12] H. S. Han *et al.*, "Current status and outlook on the clinical translation of biodegradable metals," *Mater. Today*, vol. 23, no. March, pp. 57–71, 2019.

[13] Y. Yang *et al.*, "Mg bone implant: Features, developments and perspectives," *Mater. Des.*, vol. 185, p. 108259, 2020.

[14] S. M. Glasdam, S. Glasdam, and G. H. Peters, “The Importance of Magnesium in the Human Body: A Systematic Literature Review,” *Adv. Clin. Chem.*, vol. 73, pp. 169–193, 2016.

[15] N. E. L. Saris, E. Mervaala, H. Karppanen, J. A. Khawaja, and A. Lewenstam, “Magnesium: An update on physiological, clinical and analytical aspects,” *Clin. Chim. Acta*, vol. 294, no. 1–2, pp. 1–26, 2000.

[16] P. C. Banerjee, S. Al-Saadi, L. Choudhary, S. E. Harandi, and R. Singh, “Magnesium implants: Prospects and challenges,” *Materials (Basel).*, vol. 12, no. 1, pp. 1–21, 2019.

[17] J. Chen, L. Tan, X. Yu, I. P. Etim, M. Ibrahim, and K. Yang, “Mechanical properties of magnesium alloys for medical application: A review,” *J. Mech. Behav. Biomed. Mater.*, vol. 87, no. July, pp. 68–79, 2018.

[18] J. L. Wang, J. K. Xu, C. Hopkins, D. H. K. Chow, and L. Qin, “Biodegradable Magnesium-Based Implants in Orthopedics—A General Review and Perspectives,” *Adv. Sci.*, vol. 7, no. 8, 2020.

[19] M. P. Staiger, A. M. Pietak, J. Huadmai, and G. Dias, “Magnesium and its alloys as orthopedic biomaterials: A review,” *Biomaterials*, vol. 27, no. 9, pp. 1728–1734, 2006.

[20] S. Castiglioni, A. Cazzaniga, W. Albisetti, and J. A. M. Maier, “Magnesium and osteoporosis: Current state of knowledge and future research directions,” *Nutrients*, vol. 5, no. 8, pp. 3022–3033, 2013.

[21] M. Li, P. Wan, W. Wang, K. Yang, Y. Zhang, and Y. Han, “Regulation of osteogenesis and osteoclastogenesis by zoledronic acid loaded on biodegradable magnesium-strontium alloy,” *Sci. Rep.*, vol. 9, no. 1, pp. 1–12, 2019.

[22] F. Witte, “Reprint of: The history of biodegradable magnesium implants: A review,” *Acta Biomater.*, vol. 23, no. S, pp. S28–S40, 2015.

[23] K. Jähn *et al.*, *Intramedullary Mg2Ag nails augment callus formation during fracture healing in mice*, vol. 36. Acta Materialia Inc., 2016.

[24] The Editors of Encyclopaedia Britannica, “Callus,” *Encyclopædia Britannica, inc.*, 2007. [Online]. Available: https://www.britannica.com/science/callus-osteology. [Accessed: 23-Dec-2019].

[25] F. Witte *et al.*, “In vivo corrosion of four magnesium alloys and the associated bone response,” *Biomaterials*, vol. 26, no. 17, pp. 3557–3563, 2005.

[26] G. Chandra and A. Pandey, “Preparation Strategies for Mg-alloys for Biodegradable Orthopaedic Implants and Other Biomedical Applications: A Review,” *Irbm*, vol. 1, pp. 1–21, 2020.

[27] J. Niu *et al.*, “The in vivo degradation and bone-implant interface of Mg-Nd-Zn-Zr alloy screws: 18 months post-operation results,” *Corros. Sci.*, vol. 113, pp. 183–187, 2016.

[28] W. M. M. Thomas P. Ruedi, “AO Principles of Fracture Management,” in *AO Principles of Fracture Managment*, Thieme Medical Publishers, 2001, pp. 7–33.

[29] D. Persaud-Sharma and A. Mcgoron, “Biodegradable magnesium alloys: A review of material development and applications,” *J. Biomim. Biomater. Tissue Eng.*, vol. 12, no. 1, pp. 25–39, 2012.

[30] R. Zeng, W. Dietzel, F. Witte, N. Hort, and C. Blawert, “Progress and challenge for magnesium alloys as biomaterials,” *Adv. Eng. Mater.*, vol. 10, no. 8, pp. 3–14, 2008.

[31] G. Eddy Jai Poinern, S. Brundavanam, and D. Fawcett, “Biomedical Magnesium Alloys: A Review of Material Properties, Surface Modifications and Potential as a Biodegradable Orthopaedic Implant,” *Am. J. Biomed. Eng.*, vol. 2, no. 6, pp. 218–240, 2013.

[32] W. D. Mueller, M. F. Lorenzo De Mele, M. L. Nascimento, and M. Zeddies, “Degradation of magnesium and its alloys: Dependence on the composition of the synthetic biological media,” *J. Biomed. Mater. Res. - Part A*, vol. 90, no. 2, pp. 487–495, 2009.

[33] L. Li, M. Zhang, Y. Li, J. Zhao, L. Qin, and Y. Lai, “Corrosion and biocompatibility improvement of magnesium-based alloys as bone implant materials: A review,” *Regen. Biomater.*, vol. 4, no. 2, pp. 129–137, 2017.

[34] G. Song, “Control of biodegradation of biocompatable magnesium alloys,” *Corros. Sci.*, vol. 49, no. 4, pp. 1696–1701, 2007.

[35] R. Karunakaran, S. Ortgies, A. Tamayol, F. Bobaru, and M. P. Sealy, “Additive manufacturing of magnesium alloys,” *Bioact. Mater.*, vol. 5, no. 1, pp. 44–54, 2020.

[36] Y. Chen, Z. Xu, C. Smith, and J. Sankar, “Recent advances on the development of magnesium alloys for biodegradable implants,” *Acta Biomater.*, vol. 10, no. 11, pp. 4561–4573, 2014.

[37] Z. Wei, P. Tian, X. Liu, and B. Zhou, “In vitro degradation, hemolysis, and cytocompatibility of PEO/PLLA composite coating on biodegradable AZ31 alloy,” *J. Biomed. Mater. Res. - Part B Appl. Biomater.*, vol. 103, no. 2, pp. 342–354, 2015.

[38] T. M. Mukhametkaliyev *et al.*, “A biodegradable AZ91 magnesium alloy coated with a thin nanostructured hydroxyapatite for improving the corrosion resistance,” *Mater. Sci. Eng. C*, vol. 75, pp. 95–103, 2017.

[39] X. Gu, Y. Zheng, Y. Cheng, S. Zhong, and T. Xi, “In vitro corrosion and

biocompatibility of binary magnesium alloys," *Biomaterials*, vol. 30, no. 4, pp. 484–498, 2009.

[40] Y. Ding, C. Wen, P. Hodgson, and Y. Li, "Effects of alloying elements on the corrosion behavior and biocompatibility of biodegradable magnesium alloys: A review," *J. Mater. Chem. B*, vol. 2, no. 14, pp. 1912–1933, 2014.

[41] J. Liu *et al.*, "Comparative in vitro study on binary Mg-RE (Sc, Y, La, Ce, Pr, Nd, Sm, Eu, Gd, Tb, Dy, Ho, Er, Tm, Yb and Lu) alloy systems," *Acta Biomater.*, vol. 102, pp. 508–528, 2020.

[42] Z. Li, X. Gu, S. Lou, and Y. Zheng, "The development of binary Mg-Ca alloys for use as biodegradable materials within bone," *Biomaterials*, vol. 29, no. 10, pp. 1329–1344, 2008.

[43] A. Mohamed, A. M. El-Aziz, and H. G. Breitinger, "Study of the degradation behavior and the biocompatibility of Mg–0.8Ca alloy for orthopedic implant applications," *J. Magnes. Alloy.*, vol. 7, no. 2, pp. 249–257, 2019.

[44] H. Hornberger, S. Virtanen, and A. R. Boccaccini, "Biomedical coatings on magnesium alloys - A review," *Acta Biomater.*, vol. 8, no. 7, pp. 2442–2455, 2012.

[45] Z. Z. Yin *et al.*, "Advances in coatings on biodegradable magnesium alloys," *J. Magnes. Alloy.*, no. xxxx, 2020.

[46] M. Rahman, N. K. Dutta, and N. Roy Choudhury, "Magnesium Alloys With Tunable Interfaces as Bone Implant Materials," *Front. Bioeng. Biotechnol.*, vol. 8, no. June, 2020.

[47] S. V. Dorozhkin, "Calcium orthophosphate coatings on magnesium and its biodegradable alloys," *Acta Biomater.*, vol. 10, no. 7, pp. 2919–2934, 2014.

[48] R. G. Guan *et al.*, "Electrodeposition of hydroxyapatite coating on Mg-4.0Zn-1.0Ca-0.6Zr alloy and in vitro evaluation of degradation, hemolysis, and cytotoxicity," *J. Biomed. Mater. Res. - Part A*, vol. 100 A, no. 4, pp. 999–1015, 2012.

[49] K. J. L. Burg, S. Porter, and J. F. Kellam, "Biomaterial developments for bone tissue engineering," *Biomaterials*, vol. 21, no. 23, pp. 2347–2359, 2000.

[50] S. Samavedi, A. R. Whittington, and A. S. Goldstein, "Calcium phosphate ceramics in bone tissue engineering: A review of properties and their influence on cell behavior," *Acta Biomater.*, vol. 9, no. 9, pp. 8037–8045, 2013.

[51] M. A. Surmeneva and R. A. Surmenev, "Microstructure characterization and corrosion behaviour of a nano-hydroxyapatite coating deposited on AZ31 magnesium alloy using radio frequency magnetron sputtering," *Vacuum*, vol. 117, pp. 60–62, 2015.

[52] V. S. Yadav, A. Kumar, A. Das, D. Pamu, L. M. Pandey, and M. R. Sankar, "Degradation kinetics and surface properties of bioceramic hydroxyapatite coated AZ31 magnesium alloys for biomedical applications," *Mater. Lett.*, vol. 270, p. 127732, 2020.

[53] R. G. Guan *et al.*, "Electrodeposition of hydroxyapatite coating on Mg-4.0Zn-1.0Ca-0.6Zr alloy and in vitro evaluation of degradation, hemolysis, and cytotoxicity," *J. Biomed. Mater. Res. - Part A*, vol. 100 A, no. 4, pp. 999–1015, 2012.

[54] G. Peluso, O. Petillo, L. Ambrosio, and L. Nicolais, "Polyetherimide as biomaterial: preliminary in vitro and in vivo biocompatibility testing," *J. Mater. Sci. Mater. Med.*, vol. 5, no. 9–10, pp. 738–742, 1994.

[55] N. Scharnagl, C. Blawert, and W. Dietzel, "Corrosion protection of magnesium alloy AZ31 by coating with poly(ether imides) (PEI)," *Surf. Coatings Technol.*, vol. 203, no. 10–11, pp. 1423–1428, 2009.

[56] T. F. Conceicao, N. Scharnagl, C. Blawert, W. Dietzel, and K. U. Kainer, "Corrosion protection of magnesium alloy AZ31 sheets by spin coating process with poly(ether imide) [PEI]," *Corros. Sci.*, vol. 52, no. 6, pp. 2066–2079, 2010.

[57] S. B. Kim, J. H. Jo, S. M. Lee, H. E. Kim, K. H. Shin, and Y. H. Koh, "Use of a poly(ether imide) coating to improve corrosion resistance and biocompatibility of magnesium (Mg) implant for orthopedic applications," *J. Biomed. Mater. Res. - Part A*, vol. 101 A, no. 6, pp. 1708–1715, 2013.

[58] E. Hart, "Corrosion inhibitors: Principles, mechanisms and applications," *Corros. Inhib. Princ. Mech. Appl.*, pp. 1–161, 2016.

[59] L. Li, F. Pan, and J. Lei, "Environmental Friendly Corrosion Inhibitors for Magnesium Alloys," *Magnes. Alloy. - Corros. Surf. Treat.*, 2011.

[60] A. S. Gnedenkov, S. L. Sinebryukhov, D. V. Mashtalyar, and S. V. Gnedenkov, "Protective properties of inhibitor-containing composite coatings on a Mg alloy," *Corros. Sci.*, vol. 102, pp. 348–354, 2016.

[61] G. Chindamo, S. Sapino, E. Peira, D. Chirio, M. C. Gonzalez, and M. Gallarate, "Bone diseases: Current approach and future perspectives in drug delivery systems for bone targeted therapeutics," *Nanomaterials*, vol. 10, no. 5, 2020.

[62] R. Rothe *et al.*, "Adjuvant drug-assisted bone healing: Advances and challenges in drug delivery approaches," *Pharmaceutics*, vol. 12, no. 5, pp. 1–41, 2020.

[63] S. Young, M. Wong, Y. Tabata, and A. G. Mikos, "Gelatin as a delivery vehicle for the controlled release of bioactive molecules," *J. Control. Release*, vol. 109, no. 1–3, pp. 256–274, 2005.

[64] G. Carriers, F. O. R. Drug, and C. D. In, “NIH Public Access GELATIN CARRIERS FOR DRUG AND CELL DELIVERY IN,” no. 713, pp. 210–218, 2015.

[65] M. Foox and M. Zilberman, “Drug delivery from gelatin-based systems,” *Expert Opin. Drug Deliv.*, vol. 12, no. 9, pp. 1547–1563, 2015.

[66] B. V. Parakhonskiy *et al.*, “Macromolecule Loading into Spherical, Elliptical, Star-Like and Cubic Calcium Carbonate Carriers,” *ChemPhysChem*, vol. 15, no. 13, pp. 2817–2822, 2014.

[67] Ç. M. Oral and B. Ercan, “Influence of pH on morphology, size and polymorph of room temperature synthesized calcium carbonate particles,” *Powder Technol.*, vol. 339, pp. 781–788, 2018.

[68] R. Salomão, L. M. M. Costa, and G. M. de Olyveira, “Precipitated Calcium Carbonate Nano-Microparticles: Applications in Drug Delivery,” *Adv. Tissue Eng. Regen. Med. Open Access*, vol. 3, no. 2, 2017.

[69] ISO 10993-1, Biological evaluation of medical devices — Part 1: Evaluation and testing within a risk management process.

[70] S. Braune, M. Grunze, A. Straub, and F. Jung, “Are there sufficient standards for the in vitro hemocompatibility testing of biomaterials?,” *Biointerphases*, vol. 8, no. 1, pp. 1–9, 2013.

[71] ISO 10993-5, Biological evaluation of medical devices- Part 5: Tests for in vitro cytotoxicity.

[72] ISO 10993-12, Biological evaluation of medical devices - Part 12: Sample preparation and reference materials.

[73] Cayman chemical, “LDH Cytotoxicity Assay Kit,” *New York, Harper Row*, no. 601170, pp. 1–19, 2016.

[74] M. A. T. Freeberg, J. G. Kallenbach, and H. A. Awad, *Assessment of cellular responses of tissue constructs in vitro in regenerative engineering*, vol. 1–3. Elsevier, 2019.

[75] ISO10993-4, Biological evaluation of medical devices - Part 4: Selection of tests for interactions with blood.

[76] M. Weber *et al.*, “Blood-Contacting Biomaterials: In Vitro Evaluation of the Hemocompatibility,” *Front. Bioeng. Biotechnol.*, vol. 6, no. July, 2018.

[77] W. van Oeveren, “Obstacles in Haemocompatibility Testing,” *Scientifica (Cairo).*, vol. 2013, pp. 1–14, 2013.

[78] C. Sperling, M. F. Maitz, and C. Werner, *Test methods for hemocompatibility of biomaterials*. Elsevier Ltd., 2018.

[79] B. D. Ratner and T. A. Horbett, *Evaluation of Blood-Materials Interactions*, Third Edit. Elsevier, 2013.

[80] Y. Wo, E. J. Brisbois, R. H. Bartlett, and M. E. Meyerhoff, "Recent advances in thromboresistant and antimicrobial polymers for biomedical applications: just say yes to nitric oxide (NO)," *Biomater. Sci.*, vol. 4, no. 8, pp. 1161–1183, 2016.

[81] P. Nesargikar, B. Spiller, and R. Chavez, "The complement system: History, pathways, cascade and inhibitors," *Eur. J. Microbiol. Immunol.*, vol. 2, no. 2, pp. 103–111, 2012.

[82] A. Myrissa *et al.*, "In vitro and in vivo comparison of binary Mg alloys and pure Mg," *Mater. Sci. Eng. C*, vol. 61, pp. 865–874, 2016.

[83] Z. Li, Z. Shang, X. Wei, and Q. Zhao, "Corrosion resistance and cytotoxicity of AZ31 magnesium alloy with N+ ion implantation," *Mater. Technol.*, vol. 34, no. 12, pp. 730–736, 2019.

[84] P. Makkar, H. J. Kang, A. R. Padalhin, O. Faruq, and B. T. Lee, "In-vitro and in-vivo evaluation of strontium doped calcium phosphate coatings on biodegradable magnesium alloy for bone applications," *Appl. Surf. Sci.*, vol. 510, no. June 2019, p. 145333, 2020.

[85] Y. Guo *et al.*, "Enhanced corrosion resistance and biocompatibility of polydopamine/dicalcium phosphate dihydrate/collagen composite coating on magnesium alloy for orthopedic applications," *J. Alloys Compd.*, vol. 817, p. 152782, 2020.

[86] J. Tian *et al.*, "Investigation of the antimicrobial activity and biocompatibility of magnesium alloy coated with HA and antimicrobial peptide," *J. Mater. Sci. Mater. Med.*, vol. 26, no. 2, 2015.

[87] X. Liu *et al.*, "Microstructure, mechanical properties, in vitro degradation behavior and hemocompatibility of novel Zn-Mg-Sr alloys as biodegradable metals," *Mater. Lett.*, vol. 162, pp. 242–245, 2016.

[88] D. Zhao, F. Witte, F. Lu, J. Wang, J. Li, and L. Qin, "Current status on clinical applications of magnesium-based orthopaedic implants: A review from clinical translational perspective," *Biomaterials*, vol. 112, pp. 287–302, 2017.

[89] R. Biber, J. Pauser, M. Geßlein, and H. J. Bail, "Magnesium-Based Absorbable Metal Screws for Intra-Articular Fracture Fixation," *Case Rep. Orthop.*, vol. 2016, pp. 1–4, 2016.

[90] J. M. Seitz, A. Lucas, and M. Kirschner, "Magnesium-Based Compression Screws: A Novelty in the Clinical Use of Implants," *Jom*, vol. 68, no. 4, pp. 1177–1182, 2016.

[91] J. T. Choo, S. H. S. Lai, C. Q. Y. Tang, and G. Thevendran, "Magnesium-based

bioabsorbable screw fixation for hallux valgus surgery – A suitable alternative to metallic implants," *Foot Ankle Surg.*, vol. 25, no. 6, pp. 727–732, 2019.

[92] H. Leonhardt, A. Franke, N. M. H. McLeod, G. Lauer, and A. Nowak, "Fixation of fractures of the condylar head of the mandible with a new magnesium-alloy biodegradable cannulated headless bone screw," *Br. J. Oral Maxillofac. Surg.*, vol. 55, no. 6, pp. 623–625, 2017.

[93] D. Zhao *et al.*, "Vascularized bone grafting fixed by biodegradable magnesium screw for treating osteonecrosis of the femoral head," *Biomaterials*, vol. 81, pp. 84–92, 2016.

[94] J. W. Lee *et al.*, "Long-term clinical study and multiscale analysis of in vivo biodegradation mechanism of Mg alloy," *Proc. Natl. Acad. Sci. U. S. A.*, vol. 113, no. 3, pp. 716–721, 2016.

[95] L. Chen *et al.*, "Treatment of trauma-induced femoral head necrosis with biodegradable pure Mg screw-fixed pedicle iliac bone flap," *J. Orthop. Transl.*, vol. 17, pp. 133–137, 2019.

[96] B. Acar, O. Kose, A. Turan, M. Unal, Y. A. Kati, and F. Guler, "Comparison of Bioabsorbable Magnesium versus Titanium Screw Fixation for Modified Distal Chevron Osteotomy in Hallux Valgus," *Biomed Res. Int.*, vol. 2018, 2018.

[97] K. S. Park, C. Kim, J. O. Nam, S. M. Kang, and C. S. Lee, "Synthesis and characterization of thermosensitive gelatin hydrogel microspheres in a microfluidic system," *Macromol. Res.*, vol. 24, no. 6, pp. 529–536, 2016.

[98] Y. Wang, Y. X. Moo, C. Chen, P. Gunawan, and R. Xu, "Fast precipitation of uniform $CaCO_3$ nanospheres and their transformation to hollow hydroxyapatite nanospheres," *J. Colloid Interface Sci.*, vol. 352, no. 2, pp. 393–400, 2010.

[99] J. Yu, M. Lei, and B. Cheng, "Facile preparation of monodispersed calcium carbonate spherical particles via a simple precipitation reaction," *Mater. Chem. Phys.*, vol. 88, no. 1, pp. 1–4, 2004.

[100] A. C. Estrada, A. L. Daniel-Da-Silva, and T. Trindade, "Photothermally enhanced drug release by κ-carrageenan hydrogels reinforced with multi-walled carbon nanotubes," *RSC Adv.*, vol. 3, no. 27, pp. 10828–10836, 2013.

[101] ASTM, "Standard Practice for Assessment of Hemolytic Properties of Materials 1," *Practice*, vol. i, pp. 1–5, 2013.

[102] R. Dinarvand, S. Mahmoodi, E. Farboud, M. Salehi, and F. Atyabi, "Preparation of gelatin microspheres containing lactic acid - Effect of cross-linking on drug release," *Acta Pharm.*, vol. 55, no. 1, pp. 57–67, 2005.

[103] D. B. Trushina, T. V. Bukreeva, and M. N. Antipina, “Size-Controlled Synthesis of Vaterite Calcium Carbonate by the Mixing Method: Aiming for Nanosized Particles,” *Cryst. Growth Des.*, vol. 16, no. 3, pp. 1311–1319, 2016.

[104] A. Declet, E. Reyes, and O. M. Suárez, “Calcium carbonate precipitation: A review of the carbonate crystallization process and applications in bioinspired composites,” *Rev. Adv. Mater. Sci.*, vol. 44, no. 1, pp. 87–107, 2016.

[105] P. E. Bunney, A. N. Zink, A. A. Holm, C. J. Billington, and C. M. Kotz, “Metabolic regulation of cell growth and proliferation,” *Physiol. Behav.*, vol. 176, no. 5, pp. 139–148, 2017.

[106] T. Capiod, “The Need for Calcium Channels in Cell Proliferation,” *Recent Pat. Anticancer. Drug Discov.*, vol. 8, no. 1, pp. 4–17, 2012.

[107] J. P. I. Sousa, C. S. Neves, J. Pereira, A.C. Bastos, L. Moreira, S. Fraga, “Multilayer coatings for corrosion protection of Mg alloys used in biomedical applications,” *EUROCORR*. 2020.

[108] P. Xiong *et al.*, “Osteogenic and pH stimuli-responsive self-healing coating on biomedical Mg-1Ca alloy,” *Acta Biomater.*, vol. 92, pp. 336–350, 2019.

[109] A. Abdal-Hay, N. A. M. Barakat, and J. K. Lim, “Hydroxyapatite-doped poly(lactic acid) porous film coating for enhanced bioactivity and corrosion behavior of AZ31 Mg alloy for orthopedic applications,” *Ceram. Int.*, vol. 39, no. 1, pp. 183–195, 2013.

[110] P. Sikder, Y. Ren, and S. B. Bhaduri, “Synthesis and evaluation of protective poly(lactic acid) and fluorine-doped hydroxyapatite-based composite coatings on AZ31 magnesium alloy,” *J. Mater. Res.*, vol. 34, no. 22, pp. 3766–3776, 2019.

[111] B. Lin *et al.*, “Preparation and characterization of dopamine-induced biomimetic hydroxyapatite coatings on the AZ31 magnesium alloy,” *Surf. Coatings Technol.*, vol. 281, pp. 82–88, 2015.

[112] G. Parande *et al.*, “Strength retention, corrosion control and biocompatibility of Mg–Zn–Si/HA nanocomposites,” *J. Mech. Behav. Biomed. Mater.*, vol. 103, p. 103584, 2020.

[113] S. B. Kim, J. H. Jo, S. M. Lee, H. E. Kim, K. H. Shin, and Y. H. Koh, “Use of a poly(ether imide) coating to improve corrosion resistance and biocompatibility of magnesium (Mg) implant for orthopedic applications,” *J. Biomed. Mater. Res. - Part A*, vol. 101 A, no. 6, pp. 1708–1715, 2013.

[114] X. L. Liu, W. R. Zhou, Y. H. Wu, Y. Cheng, and Y. F. Zheng, “Effect of sterilization process on surface characteristics and biocompatibility of pure Mg and MgCa alloys,”

Mater. Sci. Eng. C, vol. 33, no. 7, pp. 4144–4154, 2013.

[115] C. H. Ooi, Y. P. Ling, W. Z. Abdullah, A. Z. Mustafa, S. Y. Pung, and F. Y. Yeoh, "Physicochemical evaluation and in vitro hemocompatibility study on nanoporous hydroxyapatite," *J. Mater. Sci. Mater. Med.*, vol. 30, no. 4, 2019.

[116] B. I. Cerda-Cristerna, H. Flores, A. Pozos-Guillén, E. Pérez, C. Sevrin, and C. Grandfils, "Hemocompatibility assessment of poly(2-dimethylamino ethylmethacrylate) (PDMAEMA)-based polymers," *J. Control. Release*, vol. 153, no. 3, pp. 269–277, 2011.

[117] Z. Zhen, X. Liu, T. Huang, T. Xi, and Y. Zheng, "Hemolysis and cytotoxicity mechanisms of biodegradable magnesium and its alloys," *Mater. Sci. Eng. C*, vol. 46, pp. 202–206, 2015.

[118] Q. Wang, L. Tan, and K. Yang, "Cytocompatibility and Hemolysis of AZ31B Magnesium Alloy with Si-containing Coating," *J. Mater. Sci. Technol.*, vol. 31, no. 8, pp. 845–851, 2015.

[119] S. Singh, G. Singh, and N. Bala, "Electrophoretic deposition of Fe 3 O 4 nanoparticles incorporated hydroxyapatite-bioglass-chitosan nanocomposite coating on AZ91 Mg alloy," *Mater. Today Commun.*, no. April, p. 101870, 2020.

[120] N. Sahoo, R. K. Sahoo, N. Biswas, A. Guha, and K. Kuotsu, "Recent advancement of gelatin nanoparticles in drug and vaccine delivery," *Int. J. Biol. Macromol.*, vol. 81, pp. 317–331, 2015.